EXPERIMENTAL DIABETIC NEPHROPATHY CAN BE AMELIORATED USING TRANSGLUTAMINASE INHIBITORS

Short Title: -- Transglutaminase Inhibition in Diabetic Nephropathy

Linghong Huang[1], John L. Haylor[1], Zoe Hau[1], Richard Jones[2*], Melissa E. Vickers[1], Bart Wagner[3], Martin Griffin[4], Robert E. Saint[2], Ian G.C. Coutts[2], A. Meguid El Nahas[1] and Timothy S. Johnson[1]

[1] *Academic Nephrology Unit, Sheffield Kidney Institute (University of Sheffield), Sheffield, UK*
[2] *School of Science and Mathematics, Nottingham Trent University, Nottingham, UK*
[3] *Department of Histology, Northern General Hospital, Sheffied UK*
[4] *School of Life and Health Sciences, Aston University, Birmingham, UK*

Corresponding Author
Dr. Tim Johnson BSc PhD
Academic Nephrology Unit (Sheffield Kidney Institute), Room GU24
School of Medicine & Biomedical Sciences (The University of Sheffield)
Royal Hallamshire Hospital, Beech Hill Road
Sheffield, S10 2RZ, United Kingdom
Tel: +44 (0)114 2712842
Fax: +44 (0)114 2711711
Email: t.johnson@sheffield.ac.uk

Abstract

Diabetic nephropathy (DN) is characterized by excessive extracellular matrix (ECM) accumulation that results in renal scarring leading to end stage kidney failure. Previous studies suggest that tissue transglutaminase (TG2) through formation of its protein crosslink product, ε-(γ-glutamyl) lysine, alters ECM homeostasis and causes basement membrane thickening and expansion of the mesangium and interstitium. To determine if transglutaminase (TG) inhibition was able to slow the progression of chronic experimental DN over an extended treatment period, TG inhibitor NTU281 was applied to streptozotocin (STZ)-induced diabetic uninephrectomy rats for up to 8 months.

Effective TG inhibition reduced the increases in serum creatinine (-68%) and albuminuria (-80%) in the diabetic rats. These improvements were accompanied by a 5 fold decrease in glomerulosclerosis and 6 fold reduction in tubulointerstitial scarring. This was associated with reduced collagen IV accumulation by 4 months, and collagen I & III by 8 months. In addition, TG inhibition lowered the numbers of myofibroblasts suggesting TG2 may play a role in myofibroblast transformation. In conclusion TG inhibition ameliorates the progression of experimental DN and can therefore be considered as a prime candidate to be developed for clinical application.

Introduction

Diabetic nephropathy (DN) is the most common cause of end-stage renal disease (ESRD) [1, 2] accounting for 50% of cases requiring renal replacement therapy (RRT) in the USA [3]. This is due to the increasing prevalence of type 2 diabetes and the reduced mortality of DN patients resulting from better management. Diabetic patients now live longer and patients with diabetic ESRD are now being accepted for treatment in dialysis programs where formerly they may have been excluded.

Clinically, the progression of DN is accompanied by the development of proteinuria and early glomerular hyperfiltration followed by a decline of glomerular filtration rate (GFR). Morphologically, it is characterised by excessive renal extracellular matrix (ECM) accumulation in the glomeruli and tubulointerstitial space causing glomerulosclerosis and tubulointerstitial fibrosis. This ultimately leads to ESRD.

TG2 is a calcium dependent enzyme that catalyzes an acyl-transfer reaction (EC 2.3.2.13) between the γ-carboxamide group of peptide-bound glutamine and the ε-amino group of peptide-bound lysine. This leads to the formation of a stable and proteolytic-resistant ε-(γ-glutamyl) lysine dipeptide bond resulting in intra- or inter-molecular crosslinks in protein. A number of extracellular proteins including fibronectin [4], collagen [5], fibrinogen [6], osteopontin [7], laminin and nidogen [8] are TG2 substrates. When TG2 is released from the cell, the high extracellular Ca^{2+} and low GTP (which modulates Ca^{2+} activation of the enzyme) activates the enzyme, enabling crosslinking of these ECM proteins at the cell surface and in the surrounding matrix. Crosslinking of collagen by TG2 has been associated with stabilisation of the collagen fibril independently of lysyl oxidase [5], accelerated ECM deposition [9], reduced proteolytic breakdown of the ECM [10] and ultimately lower ECM turnover [11]. Thus TG2 action shifts the ECM deposition-degradation balance towards

accumulation [12] and has subsequently been linked to a range of fibrogenic conditions.

A role for TG2 in the pathogenesis of DN has been reported in both the streptozotocin (STZ)-induced model of type 1 diabetes [13] and human diabetic kidney disease [14], with increased TG2 mediated ε-(γ-glutamyl) lysine crosslink formation in diabetic kidneys tightly associated with both glomerular and tubulointerstitial ECM expansion. Currently, there remains no viable mechanism for interfering with this ECM build up. Subsequently the development of therapeutic approaches directly targeting this process may provide an effective approach to the prevention of DN as well as numerous other fibrotic conditions. The inhibition of TG activity in proximal tubular epithelial cells in culture has already been shown to reduce glucose-induced ECM accumulation [15] providing strong support for *in vivo* application of such compounds in the treatment to DN. Therefore, in this study the TG site directed irreversible inhibitor N-benzyloxycarbonyl-L-phenylalanyl-6-dimethylsulfonium-5-oxo-L-norleucine (NTU281) has been applied by direct intra-renal infusion into the kidneys of rats receiving STZ injection and uninephrectomy over an 8-month treatment period. NTU281 is a benzyloxycarbonyl phenylalanyl analogue containing a dimethylsulfonium group that binds the cysteine residue in the active site of TG to instigate an acetonylation reaction leading to permanent non competitive inhibition of the enzyme [16]. Whilst the STZ model is not directly representative of DN in humans as it lacks the characteristic histological lesions, it is a useful surrogate for the impact of sustained hyperglycaemia on changes in ECM turnover in the kidney. Uninephrectomy has been used to accelerate diabetic kidney changes [17, 18]. We report TG inhibition can preserve kidney function, reduce albuminuria and ameliorate

the progression of the histological changes associated with the formation of scar tissue in DN.

Results

Verification of drug delivery

To ascertain if the intra renal cannulation was achieving uniform drug delivery throughout the kidney we prepared a dansyl labelled version of NTU281. Using a kidney that was cannulated 28 days previously (to allow the fibrous coat around the cannula to develop) and had received PBS from implant, we infused 50mM dansyl labelled NTU281 for 24 hours. Cryostat sections viewed under a fluorescent microscope demonstrated a uniform distribution of dansyl NTU281 in both the longitudinal and transverse planes in comparison to the contralateral kidney where no fluorescence was visible (Figure 1A). Import of images into multi analyst image analysis software allowed densitometric profile assessment of the fluorescence which confirmed equal distribution in both planes (Figure 1B).

Experimental groups

4 experimental groups were used. Normal, uninephrectomy (UNx), UNx + Streptozotocin (STZ) (referred to as diabetic or DM) and UNx + STZ + Transglutaminase inhibitor NTU281 (referred to as diabetic treated).

General Observations

Calculation of osmotic pump delivery rates from residual pump volumes demonstrated consistent drug delivery throughout the treatment period [Figure 2(i)]. Examination of cannulas at termination indicated all had remained *in situ* and there was no evidence of cannula leakage.

Compared to normal and UNx animals, both diabetic groups (i.e. treated & untreated with NTU281) had higher levels of blood glucose throughout the experimental period [Figure 2 (iii)], and within the 10-25 mmol/L target range using a comparable insulin

dose [Figure 2(ii)] thus demonstrating an equal metabolic burden in treated and untreated rats.

In hyperglycaemic animals by 8 months post STZ, body weight gain was approximately 2 fold lower [Figure 2(iv)] than in normal rats reaching 355±12.8g and 377±14.3g in diabetic and NTU281 treated diabetic rats respectively compared to 546±22.6g in normal (Table 1).

Kidney weight following UNx was greater than normal, but only significantly at 1 month post STZ (Table 1). Imposing hyperglycaemia caused a marked increase in kidney weight being more than 3 fold greater by 8 months, however TG inhibition reduced increased kidney weight by 42% at this point (Table 1).

Although blood pressure was raised in hyperglycaemic animals, there was no significant difference in systolic blood pressure between the 4 groups through the study (not shown).

Effectiveness of TG Inhibition

TG *in situ* activity assays showed a 6-fold increase in extracellular TG activity in the untreated diabetic animals by 8 months [Figure 3(i)]. Increased extracellular TG activity was present both in the glomeruli and tubulointerstitial compartments [Figure 3(ii)]. In comparison, the extracellular TG activity in the NTU281-treated diabetic rats remained similar to that in both normal and uninephrectomy (UNx) controls throughout [Figure 3(i)]. In agreement with less extracellular TG activity in treated animals were lower levels of catalysed ε-(γ-glutamyl) lysine crosslinking (P<0.05) which were unaltered compared to the normal and UNx controls throughout the experimental period [Figure 3(iii)] demonstrating continuous effective TG inhibition.

Kidney Function and Albuminuria

Kidney function was assessed using serum creatinine. In untreated diabetic animals, serum creatinine rose throughout the experimental period with more than a 3.5-fold increase by 8 months compared to controls [Figure 2 (v)]. Although a small increase in serum creatinine ($P<0.05$) was detected in the NTU281-treated diabetic rats by 8 months, this was 68.0% lower than those receiving no treatment ($P<0.05$).

Measurement of 24-hour albumin excretion showed substantial increases in both treated and untreated diabetic groups by 4 months ($P<0.05$) that progressively increased at 8 months ($P<0.05$). However, in NTU281-treated animals the increase in 24-hour albumin excretion was lowered by approximately 80% at the end point [Figure 2 (vi)] suggesting that TG inhibition slows down the deterioration of glomerular structure and function.

Kidney Scarring and Morphology

After 1 month of hyperglycaemia, there was no substantial difference morphologically between the four experimental groups (Figure 4A-D). By 4 months, kidney hypertrophy was well established in the UNx, treated and untreated diabetic kidneys with the largest increment occurring in the diabetic groups (Figure 4E-H). Furthermore, in the untreated diabetic kidney, both tubular atrophy as well as peritubular fibrosis was noted (Figure 4G).

No evidence of interstitial fibrosis was seen at 8 months in the normal (Figure 4I) and UNx (Figure 4J) kidneys. In comparison, in the untreated diabetic kidney (Figure 4K), there was extensive epithelial flattening, tubular atrophy and interstitial expansion with severe tubulointerstitial scarring. Nearly all glomeruli showed advanced glomerulosclerosis with Bowman's space filled with collagen. There was

extensive expansion of the mesangial matrix, the capillary network had collapsed and the glomeruli were extensively vacuolated. In comparison, all these changes were dramatically reduced in the NTU281 treated diabetic kidneys (Figure 4L), with only mild focal tubular epithelial flattening and some minor expansion of the tubular basement membrane.

Transmission electron microscopy of glomeruli in 8 month kidneys demonstrated significant widespread changes in both the glomerular basement membrane (GBM) and podocytes in untreated diabetic kidneys (Figure 5A). There was a visible thickening of the GBM and most noticeably an effacement /loss of the podocytes especially visible at high power (Figure 5B). Tg inhibition prevented the effacement / loss of podocytes while computerised morphometric assessment of GBM thickness demonstrated the diabetic induced GBM thickening was prevented with TG inhibition (Figure 5C).

Quantification of Kidney Scarring

Computerised multiphase image analysis was used to assess the degree of kidney scarring on Masson's Trichrome stained sections. Assessment of glomerulosclerosis [Figure 6(i)] showed a significant increase in the level of fibrous tissue present by 4 months post hyperglycaemia that progressed significantly by 8 months in untreated diabetic kidneys being 5 fold that in control groups. NTU281 treated kidneys showed no significant increase in glomerulosclerosis compared to normal and UNx glomeruli over the 8 month period.

Tubulointerstitial fibrosis showed a similar trend to glomerulosclerosis with 2 fold increase in scarring at 4 months rising to 6 fold by 8 months in untreated diabetic animals [Figure 6(ii)]. NTU281 significantly reduced scarring in diabetic kidneys

with no detectable change compared to control at 4 months and only a 2 fold increase by 8 months.

Kidney Collagen Content

Whole kidney collagen was undertaken by measuring hydroxyproline in hydrolysed kidney homogenates.   By 8 months post STZ, the hydroxproline constituted 0.89±0.04% of total amino acids in untreated hyperglycaemic kidneys and double those in normal (0.42±0.03%) and UNx animals (0.48±0.03%). In NTU281 treated diabetic kidneys, hydroxyproline rose by just half that in the untreated diabetics reaching 0.67±0.03%.

Changes in collagens, type I, III and IV were investigated by immunofluorescense. In early experimental DN (1 and 4 months), there was no significant change in either collagen I [Figure 7(i)] or III [Figure 7(ii)] staining in the kidney between the 4 experimental groups. By 8 months, both collagen I [Figure 7(i)] and III [Figure 7(ii)] were elevated in the untreated diabetic kidney (P<0.05). Increased collagen I was mainly found in sclerotic glomeruli (Figure 8C) while elevated collagen III occurred in the expanded interstitium and in periglomerular areas (Figure 8G). In contrast, levels of both collagens in the NTU281 treated diabetic kidney remained similar to normal. Collagen IV was significantly increased by 4 months in the untreated diabetic kidney (P<0.05) and continued to increase predominantly in peritubular and periglomerular areas (Figure 8K) at 8 months (P<0.05). NTU281 treated diabetic kidneys had collagen IV staining levels that were comparable to the normal and UNx animals throughout experimental period [Figure 7(iii)].

Levels of kidney scarring significantly correlated with changes in accumulation of collagen I (r=0.515, P<0.01), collagen III (r=0.718, P<0.01) and collagen IV (r=0.570, P<0.01).

mRNA Levels of Collagen I, III and IV

To detect if the TG inhibition had an effect on collagen synthesis, Northern blotting was performed using 4 and 8-month kidneys.

At 4 months, collagen I mRNA levels in the treated diabetic kidney were similar to normal, but higher than the UNx and untreated diabetic kidneys [Figure 9(i)]. By 8 months, collagen I mRNA levels in diabetic kidneys were significantly higher than that in the normal and UNx [Figure 9(i)]. The NTU281 treated kidney had levels not significantly different from the untreated diabetic kidney [Figure 9(i)].

The collagen III mRNA levels in the untreated diabetic kidney reached 5 fold higher than those in the normal and UNx by 8 months [Figure 9(ii)]. In contrast, the levels in the NTU281 treated kidney were normalised at this stage, although they had been higher than those in the untreated diabetic kidney at the earlier time point [Figure 9(ii)].

The collagen IV mRNA levels in both treated and untreated diabetic groups were similar and higher than the UNx at 4 months post STZ administration [Figure 9(iii)]. By 8 months, it was significantly increased in the untreated diabetic kidney compared to the other 3 experimental groups with the levels more than double normal [Figure 9(iii), P<0.05]. Although the treated group had levels higher than the normal, it was not significant [Figure 9(iii)].

Overall, the above results suggested that the TG inhibitor, NTU281, had minimal effect on collagen I mRNA levels, but reduced the collagen III and IV mRNA levels by the end of the study.

Myofibroblasts (α-Smooth Muscle Actin Positive Cells)

Less interstitial cells were observed on Masson's Trichrome stained sections in the TG inhibitor treated kidney than the untreated. ECM producing myofibroblasts have been reported to be associated with the progression of fibrosis in DN [19, 20]. Therefore the abundance of these cells was determined using α-smooth muscle actin (SMA) as a marker.

At 1 month there were no substantial changes in αSMA staining between any of the experimental groups, although significant increases in α-SMA staining were detected in tubulointerstitial space of both treated and untreated diabetic kidneys by 4 months [Figure 7(iv)]. This continued to increase at 8 months [Figure 7(iv)] in the untreated group (Figure 8O). However, levels in the treated diabetic group were 67% lower than that in the untreated diabetic kidney (P<0.05) suggesting TG inhibition reduced the accumulation of myofibroblasts in advanced DN.

Discussion

All current TG inhibitors block not only TG2 activity, but also other TGs such as factor XIIIa, TG1 and TG3. Hence, there is the potential for non specific effects that could complicate data interpretation. For example, loss of keratinocyte TG (TG1) activity has been reported to cause parakeratosis and psoriasis like symptoms when applied to skin composites [21, 22] while blocking factor XIIIa may potentially lead to systemic effects such as haemorrhage and bleeding. To overcome this, we employed NTU281, an inhibitor designed to act on the outside of the cell [23] limiting its targets to TG2 and factor XIIIa which are the only two forms of mammalian TG known to be secreted into the extracellular space. Other potential targets such as cysteine proteases are in the main intracellular in nature while concentrations up to 1 mmol/L of NTU281 do not inhibit other important cysteine containing enzymes such as caspase 3. In addition, osmotic minipumps were employed to enable direct delivery of TG inhibitor to the kidney to minimise dose and hence systemic effects. Pressures generated by these pumps ensure blockage is unlikely which is supported by stable drug delivery volumes over the 8 months. Application of dansyl labelled NTU281 demonstrated uniform distribution of drug within the receiving kidney by this method. Administration of 50 mmol/L NTU281 from an implantable osmotic pump at 2.5 μl/hour to the remnant kidney in the 5/6th neprectomy (SNx) model has previously shown to halt increases in kidney TG activity without affecting blood clot stability or TG activity in other organs such as heart, liver and skin (unpublished data). Therefore, the same dose of NTU281 was used in this study and proved equally effective in reducing TG crosslinking activity in the diabetic kidney throughout the study as shown by both the reduction in TG *in situ* activity and crosslink levels which were uniform across the treated kidney.

TG inhibition resulted in preservation of kidney function and a reduction in albuminuria as a consequence of lower levels of both glomerulosclerosis and tubulointerstitial fibrosis. On commencing this study, we expected that the underlying mechanism would be related to changes in ECM accumulation by blocking the post translational processing of the ECM by extracellular TG given that *in vitro* studies have repeatedly shown that TG2 alters ECM homeostasis by accelerating the rate of collagen deposition [12] and conferring the ECM with resistance to MMP proteolysis [10]. In keeping with this we see marked reductions in mature deposited collagen I, III and IV levels in the NTU281 treated diabetic kidneys. The levels of collagen I mRNA remained high with levels between untreated and NTU281 treated groups identical In contrast, levels of collagen IV mRNA were 37% lower in the treated group and collagen III mRNA similar to normal animals by 8 months The collagen type I mRNA data clearly support a post-transcriptional mechanism (as predicted) in the presence of a continual fibrotic stimuli for collagen I, but the additional, unanticipated and interesting effect of NTU281 in suppressing type III and IV collagen mRNA levels is suggestive of an additional mechanism in lowering protein levels of these collagens.

This study was not designed to isolate particular mechanisms, and it therefore remains unclear from the data presented whether these improvements are a direct result of TG inhibition or a secondary effect caused by the reduction in fibrous tissue expansion (and thus fibrotic stimuli) brought about by lowering TGase activity. However, one could hypothesise as to 2 mechanisms that could lead to lower levels of Collagen III and IV mRNA. It has been reported that TG2 is able to activate the fibrogenic cytokine TGF-β1 by recruiting large latent TGF-β1 in the ECM prior to proteolytic release of the active dimer [24, 25]. Therefore TG inhibition may affect

collagen synthesis by simply altering latent TGF-β1 activation, and this may be the case for collagen III and IV although other *in vivo* (unpublished data) and *in vitro* [15] studies using TG inhibitors have failed to demonstrate lower active TGF-β1 levels. Alternatively, tubular ischemia caused by ECM expansion reducing blood flow to renal tubules may be less pronounced following NTU281 treatment. The reduction in levels of tubulointerstitial fibrosis in the treated diabetic kidney may therefore allow better perfusion of the tubular epithelium lowering the hypoxia-inducible factor mediated induction of ECM proteins [26].

Apart from the reduction in ECM accumulation, another marked effect of TG inhibition was the preservation of tubulointerstitial architecture with less tubular atrophy and interstitial myofibroblasts. Myofibroblasts undergo substantial proliferation and synthesize high levels of ECM proteins being central to the development of tubulointerstitial scarring and fibrosis [27-29]. Again it remains unclear from our data whether these improvements are a direct result of TG inhibition or secondary to the reduction in ECM expansion.

TG inhibition was associated with a big improvement in albuminuria indicating protection of glomerular structure. Electron microscopy of glomeruli clearly showed that TG inhibition was extremely effective in preservation of podocytes. Untreated animals had essentially no visible podocytes on the GBM indicating either loss or pedicel retraction whereas those receiving NTU281 had a podocyte structure and number that was not discernable from both control groups. The reason for this is most likely a combination of qualitative changes to the GBM (such as from the inclusion of collagen 1) and the 50% thicker GBM shown by morphometric measurements.

Lower levels of interstitial α-SMA positive cells in NTU281 treated kidneys are suggestive of a reduction in myofibroblast levels, although α-SMA is not specific for myofibroblasts with smooth muscle cells in the vasculature being particularly evident in the kidney. Epithelial-mesenchymal transdifferentiation (EMT) is thought to be a major contributor to interstitial fibrosis [30, 31] and thus a reduction in this could account for lower α-SMA staining. As previously mentioned, TG is known to play a role in latent TGF-β1 activation. Given TGF-β1 has been reported to be the most potent inducer of tubular epithelial cell EMT [32], it could be hypothesised that the increased TG activity in the diabetic kidney causes a rise in active TGF-β1 availability resulting in the activation of myofibroblast. TG inhibition may reduce the presence of myofibroblasts by blocking TG dependent TGF-β1 activation pathway [10, 13, 33].

Of note was the variation in kidney TG activity in the untreated diabetic in this model. Both control groups plus the NTU281 treated kidney showed no significant change in TG activity over the 8 months. In contrast the DM group had a 4 fold increase at 1 month, returned to near normal at 4 months with a 3 fold increase by 8 months. After repeating this assay several times we believe that this genuinely reflects a bi-phasic response of TG2. An early acute response to the hyperglycaemia which may predominantly reflect a synthesis independant cell export of TG2 as described previously in early DN [13], followed by a late remodelling response which is TG2 synthesis dependant as reported in aggressive fibrosis [10]. The discrepancy between ε(γ-glutamyl) lysine crosslink levels and TG2 activity may seem contradictory, but is not surprising. TG2 has a half life of around 8 hours so is quickly cleared while the ε(γ-glutamyl) lysine crosslink TG2 produces is very stable requiring complete

digestion of the tissue to release it. Thus if TG2 activity decreased the crosslink would remain high.

In conclusion TG inhibition dramatically slows the development of experimental DN via reduction in tubulointerstitial fibrosis and glomerulosclerosis. This preserves kidney function and slows the development of proteinuria. The prime mechanism for this is most likely to be the lowering of the direct action of TG on ECM crosslinking that leads to matrix accumulation. The data suggests that TG inhibitors offer a potential therapeutic avenue for the amelioration of DN in the diabetic patient, however clinical application is likely to be dependent on the development of isoform specific compounds.

METHODS

Synthesis of TG inhibitor

NTU281 was synthesised according to published methods [15]. Compound purity was determined by NMR and mass spectrometry. Inhibitor efficacy was verified against renal TGs by application of the inhibitor at 100 and 500μmol/L to a 20% kidney homogenate with activity measured using the [^{14}C] putrescine incorporation assay.

Experimental animals and protocol

Male Wistar Han rats (Harlan, UK) of 200 to 250g and 8 to 10 weeks old were subjected to right uninephrectomy (UNx). Seven days later hyperglycaemia was induced by tail vain injection of STZ (35mg/kg in citrate buffer, pH 4.0). Control animals were subjected to either a sham operation or UNx with vehicle injection alone. An early morning blood glucose level above 10 mmol/L at 1 week after STZ injection was considered diabetic. Blood glucose was controlled between 10 to 25 mmol/L using insulin implants (Research Pack, LinShin, Canada). Practically, 1/4 insulin implant was progressively inserted subcutaneously (using a trocar) until the target glucose range was reached. Measurements were taken 48 hours after each 1/4 implant was inserted using a One Touch Basic glucose meter (Johnson and Johnson). Blood glucose measurements were repeated biweekly with replacement implants inserted as required.

A 0.58mm bore polyethylene cannula was heat-sealed at one end and fenestrated between 2 and 12mm from the seal. The open end was attached to a 2ML4 mini osmotic pump (Alzet, USA). At UNx, the cannula was passed longitudinally through the remaining kidney such that all perforations were within the renal parenchyma. The cannula was secured using silk ties and tissue glue and run through the muscle

wall to the pump located on the scruff. Pumps were loaded with either PBS (vehicle) or 50 mmol/L solution of NTU281 and replaced every 28 days when exhausted. Rats were housed 1 to 4 to a cage at 20-22°C and 45% humidity on a 12 hours light/dark cycle. They were allowed free access to standard rat chow (Labsure Ltd., Cambridge, United Kingdom) and tap water. Animals were divided into 4 groups: normal, uninephrectomy (UNx), diabetes with UNx (UNx+DM) and diabetes with UNx treated with NTU281 (UNx+DM+NTU281). At 1, 4 and 8 months after STZ injection, rats were killed and kidneys removed from both diabetic groups (n ≥ 6) and controls (n = 4) groups. Serum creatinine was measured by standard autoanalyzer technique and 24-hour albuminuria by using the Bethyl Laboratories rat albumin ELISA kit (BioGnosis, Hailsham, UK) following the manufacturer's instructions. All procedures were carried out under license according to regulations laid down by Her Majesty's Government, United Kingdom (Animals Scientific Procedures Act, 1986).

NTU281 distribution

To ensure adequate distribution through the kidney, NTU281 was synthesised with a Dansyl label. Animals cannulated as above were infused with PBS for 1 month for the maximum fibrous coat to develop around the cannula (Figure 1A) at which stage kidneys were infused with 50mM Dansyl-NTU281 for 24 hours as above. Kidneys were removed and halved longitudinally along the cannula. Cryosections were cut at 10 μm and Dansyl visulaised under a FITC filter on a fluorescent microscope using the contralateral kidney as a control. Analysis 3.2 image analysis software (Soft imaging Systems, Germany) was used to generate a full length & width images using multi field alignement. These were imported into Multi Analyst (Biorad) and a densitometric profile generated.

Detection of In Situ TG Activity

Cryostat sections were incubated with 0.5mmol/L biotin cadaverine (Molecular Probes, Netherlands) and 5mmol/L $CaCl_2$. A negative control in which $CaCl_2$ was replaced with 10mmol/L EDTA was used. Incorporated biotin cadaverine was revealed by immunoprobing with a streptavidin indodicarbocyanine (Cy5) conjugate (Jackson ImmunoResearch, USA) at 1 in 50 dilution. Sections were visualized using a Leica TCS NT confocal microscope (Leica DMRBE; Lasertechnik, Wetzlar, Germany) using a Kr/Ar laser (647 and 488 nm) for both Cy5 (optimal excitation 650 nm) and autofluorescence. Computer imaging was obtained at 665 and 530 nm for Cy5 and autofluorescence, respectively (Leica TCS NT, Lasertechnik). Cadaverine incorporation was assessed on 6 cortical fields at 100× magnification acquired using a CC-12 digital camera (Soft Imaging Systems, Germany). Multiphase image analysis (Analysis^{TM} 3.2, Soft Imaging Systems) was performed to assess levels of incorporated cadaverine by dividing the area of red cadaverine stain with the green tissue autofluorescence to correct for tissue mass.

Detection of ε−(γ-glutamyl)-lysine Crosslink

The determination of ε−(γ-glutamyl)-lysine Crosslink was similar to previously described [13]. Cryostat sections were incubated with a mouse monoclonal anti-ε- (γ-glutamyl) lysine isopetide antibody (81-D4; Covalab, Lyon, France) or mouse nonimmune serum (DAKO) at 1 in 20 dilution. After washing and fixing, primary antibody was revealed using a donkey anti-mouse Cy5-conjugated antibody (Jackson ImmunoResearch, USA). Section visualization and multiphase image analysis were performed as described above.

Fibrosis Measurement

4μm, neutral buffered formalin fixed, paraffin embedded sections were stained with Masson's trichrome (stains collagenous material blue, nuclei, fiber, erythrocytes and elastin red/pink). For glomerulosclerosis and tubulointerstitial scarring, 20 glomeruli (400×) and 10 fields (200×) of cortex tubules were acquired respectively in a systematic manner. A fibrous coat can develop around the renal cannula which can extend up to 1 mm in thickness (Figure 1, Masons Trichrome insert). In sections immediately above or below the cannula path, affected fields are excluded from analysis to avoid data contamination. Fibrosis was assessed using multiphase image analysis [34]. The fibrosis index was determined by dividing the area of blue collagenous stain by red cellular stain thus correcting for cell number.

Immunofluorescent Measurements

Immunofluorescent staining was carried out on 4μm paraffin sections using a secondary antibody conjugated with fluorescein isothiocyanate (FITC) (DAKO). Following antigen retrieval, primary antibodies were applied as follows: goat anti-collagen (α1) III (1:10; Southern Biotech, USA), rabbit anti-collagen IV (1:35; ICN, USA) and mouse anti-αSMA (1:100, DAKO, UK). Collagen I immunofluorescence was performed on 10 μm cryostat sections using a mouse anti-collagen (α1) I antibody (1:50; Abcam, UK). Collagen IV antibodies were not chain specific recognising α1, 2, 3 and 4 chains equally.

10 cortical fields at 200× magnification of each section were acquired. These were analysed using multiphase image analysis as above with correction to DAPI staining.

Electron Microscopy

Tissue from paraffin blocks was recovered, post fixed in gluteraldehyde and subjected to transmission electron microscopy as previously described [35] using magnification

at 2600x and 20 000x. GBM thickness was determined by taking at least 10 GBM measurements per glomeruli for each animal at 20,000 magnification using Kodak AMTv600 image analysis software.

Measurement of mRNA Levels

Total RNA was extracted using TRizol^{TM} (Gibco, UK) and subjected to Northern blot analysis as previous described [36]. Autoradiographs were quantified by scanning densitometry using a Biorad GS-690 densitometer and Molecular Analyst version 4 software. Densitometry values were corrected for loading using the house keeping gene cyclophilin [36].

cDNA Probes

Specific random primed DNA probes were constructed from the following sequences: human collagen (α1) I [37], rat collagen (α1) III [38] and human collagen (α1) IV [39].

Hydroxyproline Analysis

400μl of 10% Kidney Homogenates were hydrolysed in 6M HCl at 110°C for 18 hours. These were clarified by centrifugation at 14,000rpm for 2 minutes and 20μl fractionated using a lithium chloride gradient on a Biochrom 30 amino acid analyser as optimised by the manufacturer (Biochrom, UK). Hydroxyproline was identified against an amino acid standard and expressed as a percentage of total amino acids.

Statistical Analysis

Data analyses were performed using one way ANOVA followed by a Bonferroni post hoc test. A probability of 95% ($p < 0.05$) was taken as significant. Correlation analysis was performed on SPSS 12.0.1 for Windows.

Disclosure

The patent for compound NTU281 is held by Aston University. Professor Martin Griffin is employed by Aston University and registered as an inventor on this patent. All other authors have nothing to disclose.

References

1.   Parving HH: Diabetic nephropathy: prevention and treatment. *Kidney Int* 60:2041-2055, 2001

2.   Remuzzi G, Schieppati A, Ruggenenti P: Clinical practice. Nephropathy in patients with type 2 diabetes. *N Engl J Med* 346:1145-1151, 2002

3.   Lameire N: Diabetes and diabetic nephropathy - a worldwide problem. *Acta Diabetol* 41 Suppl 1:S3-5, 2004

4.   Mosher DF: Cross-linking of fibronectin to collagenous proteins. *Mol Cell Biochem* 58:63-68, 1984

5.   Kleman JP, Aeschlimann D, Paulsson M, van der Rest M: Transglutaminase-catalyzed cross-linking of fibrils of collagen V/XI in A204 rhabdomyosarcoma cells. *Biochemistry* 34:13768-13775, 1995

6.   Martinez J, Rich E, Barsigian C: Transglutaminase-mediated cross-linking of fibrinogen by human umbilical vein endothelial cells. *J Biol Chem* 264:20502-20508, 1989

7.   Kaartinen MT, Pirhonen A, Linnala-Kankkunen A, Maenpaa PH: Cross-linking of osteopontin by tissue transglutaminase increases its collagen binding properties. *J Biol Chem* 274:1729-1735, 1999

8.   Aeschlimann D, Paulsson M: Cross-linking of laminin-nidogen complexes by tissue transglutaminase. A novel mechanism for basement membrane stabilization. *J Biol Chem* 266:15308-15317, 1991

9.   Fisher M, Huang L, Hau Z, Griffin M, El Nahas AM, Johnson TS: Over-Expression of Tissue Transglutaminase (tTg) in Proximal Tubular Epithelial (PTEC) Cells Affects ECM Accumulation In Vitro, in *Renal Association*, Belfast, Northern Ireland, UK, 2005, p 246

10. Johnson TS, Skill NJ, El Nahas AM, Oldroyd SD, Thomas GL, Douthwaite JA, Haylor JL, Griffin M: Transglutaminase transcription and antigen translocation in experimental renal scarring. *J Am Soc Nephrol* 10:2146-2157, 1999

11. Gross SR, Balklava Z, Griffin M: Importance of tissue transglutaminase in repair of extracellular matrices and cell death of dermal fibroblasts after exposure to a solarium ultraviolet A source. *J Invest Dermatol* 121:412-423, 2003

12. Fisher M, Jones RA, Huang L, Haylor JL, El Nahas M, Griffin M, Johnson TS: Modulation of tissue transglutaminase in tubular epithelial cells alters extracellular matrix levels: a potential mechanism of tissue scarring. *Matrix Biol* 28:20-31, 2009

13. Skill NJ, Griffin M, El Nahas AM, Sanai T, Haylor JL, Fisher M, Jamie MF, Mould NN, Johnson TS: Increases in renal epsilon-(gamma-glutamyl)-lysine crosslinks result from compartment-specific changes in tissue transglutaminase in early experimental diabetic nephropathy: pathologic implications. *Lab Invest* 81:705-716, 2001

14. El Nahas AM, Abo-Zenah H, Skill NJ, Bex S, Wild G, Griffin M, Johnson TS: Elevated epsilon-(gamma-glutamyl)lysine in human diabetic nephropathy results from increased expression and cellular release of tissue transglutaminase. *Nephron Clin Pract* 97:c108-117, 2004

15. Skill NJ, Johnson TS, Coutts IG, Saint RE, Fisher M, Huang L, El Nahas AM, Collighan RJ, Griffin M: Inhibition of transglutaminase activity reduces extracellular matrix accumulation induced by high glucose levels in proximal tubular epithelial cells. *J Biol Chem* 279:47754-47762, 2004

16.   Fisher M, Jones R, Griffin M, Johnson TS: Primary Tubular Epithelial Cells Isolated From The Tissue Transglutaminase Knockout Mouse Deposit Less Extracellular Matrix Than Wild Type Cells, in *Renal Associate*, Harrogate, UK, 2006, p 393

17.   Bower G, Brown DM, Steffes MW, Vernier RL, Mauer SM: Studies of the glomerular mesangium and the juxtaglomerular apparatus in the genetically diabetic mouse. *Lab Invest* 43:333-341, 1980

18.   Steffes MW, Buchwald H, Wigness BD, Groppoli TJ, Rupp WM, Rohde TD, Blackshear PJ, Mauer SM: Diabetic nephropathy in the uninephrectomized dog: microscopic lesions after one year. *Kidney Int* 21:721-724, 1982

19.   Essawy M, Soylemezoglu O, Muchaneta-Kubara EC, Shortland J, Brown CB, el Nahas AM: Myofibroblasts and the progression of diabetic nephropathy. *Nephrol Dial Transplant* 12:43-50, 1997

20.   Goumenos DS, Tsamandas AC, Oldroyd S, Sotsiou F, Tsakas S, Petropoulou C, Bonikos D, El Nahas AM, Vlachojannis JG: Transforming growth factor-beta(1) and myofibroblasts: a potential pathway towards renal scarring in human glomerular disease. *Nephron* 87:240-248, 2001

21.   Wolf R, Lo Schiavo A, Lombardi ML, Esposito C, Ruocco V: The in vitro effect of hydroxychloroquine on skin morphology and transglutaminase. *Int J Dermatol* 36:704-707, 1997

22.   Harrison CA, Gossiel F, Bullock AJ, Sun T, Blumsohn A, Mac Neil S: Investigation of keratinocyte regulation of collagen I synthesis by dermal fibroblasts in a simple in vitro model. *Br J Dermatol* 154:401-410, 2006

23.   Griffin M, Coutts I, Saint R: Dipeptide Transglutaminase Inhibitors and Methods of Using The Same, in, 2004

24.   Kojima S, Nara K, Rifkin DB: Requirement for transglutaminase in the activation of latent transforming growth factor-beta in bovine endothelial cells. *J Cell Biol* 121:439-448, 1993

25.   Nunes I, Gleizes PE, Metz CN, Rifkin DB: Latent transforming growth factor-beta binding protein domains involved in activation and transglutaminase-dependent cross-linking of latent transforming growth factor-beta. *J Cell Biol* 136:1151-1163, 1997

26.   Norman JT, Orphanides C, Garcia P, Fine LG: Hypoxia-induced changes in extracellular matrix metabolism in renal cells. *Exp Nephrol* 7:463-469, 1999

27.   Zeisberg M, Strutz F, Muller GA: Role of fibroblast activation in inducing interstitial fibrosis. *J Nephrol* 13 Suppl 3:S111-120, 2000

28.   Desmouliere A, Gabbiani G: Myofibroblast differentiation during fibrosis. *Exp Nephrol* 3:134-139, 1995

29.   Badid C, Mounier N, Costa AM, Desmouliere A: Role of myofibroblasts during normal tissue repair and excessive scarring: interest of their assessment in nephropathies. *Histol Histopathol* 15:269-280, 2000

30.   Liu Y: Epithelial to mesenchymal transition in renal fibrogenesis: pathologic significance, molecular mechanism, and therapeutic intervention. *J Am Soc Nephrol* 15:1-12, 2004

31.   Zeisberg M, Kalluri R: The role of epithelial-to-mesenchymal transition in renal fibrosis. *J Mol Med* 82:175-181, 2004

32.   Desmouliere A, Geinoz A, Gabbiani F, Gabbiani G: Transforming growth factor-beta 1 induces alpha-smooth muscle actin expression in granulation tissue myofibroblasts and in quiescent and growing cultured fibroblasts. *J Cell Biol* 122:103-111, 1993

33. Johnson TS, El-Koraie AF, Skill NJ, Baddour NM, El Nahas AM, Njloma M, Adam AG, Griffin M: Tissue transglutaminase and the progression of human renal scarring. *J Am Soc Nephrol* 14:2052-2062, 2003

34. Johnson TS, Hau Z, Fisher M, Haylor JL, Jones R, Coutts I, Saint R, El Nahas AM, Griffin M: Transglutaminase inhibition reduce renal scarring by up to 92% in the rat 5/6th subtotal nephrectomy (SNx) model, in *Renal Association*, Aberdeen, Scotland, UK, 2004, p 6

35. Yang B, Johnson TS, Thomas GL, Watson PF, Wagner B, Furness PN, El Nahas AM: A shift in the Bax/Bcl-2 balance may activate caspase-3 and modulate apoptosis in experimental glomerulonephritis. *Kidney Int* 62:1301-1313, 2002

36. Douthwaite JA, Johnson TS, Haylor JL, Watson P, El Nahas AM: Effects of transforming growth factor-beta1 on renal extracellular matrix components and their regulating proteins. *J Am Soc Nephrol* 10:2109-2119, 1999

37. Vuorio T, Makela JK, Kahari VM, Vuorio E: Coordinated regulation of type I and type III collagen production and mRNA levels of pro alpha 1(I) and pro alpha 2(I) collagen in cultured morphea fibroblasts. *Arch Dermatol Res* 279:154-160, 1987

38. Virolainen P, Perala M, Vuorio E, Aro HT: Expression of matrix genes during incorporation of cancellous bone allografts and autografts. *Clin Orthop Relat Res*:263-272, 1995

39. Kurkinen M, Condon MR, Blumberg B, Barlow DP, Quinones S, Saus J, Pihlajaniemi T: Extensive homology between the carboxyl-terminal peptides of mouse alpha 1(IV) and alpha 2(IV) collagen. *J Biol Chem* 262:8496-8499, 1987

Acknowledgements

Table

Table 1: Final body weight and terminal kidney weight.

Time / Groups	final body weight (g)			terminal kidney weight (g)		
	1-month	4-month	8-month	1-month	4-month	8-month
Normal	361±11.7	472±8.6	546±22.6	1.0±0.0	1.4±0.13	1.4±0.13
UNx	389±7.2 [a]	447±14.2	514±15.8	1.4±0.08 [a]	1.5±0.04	1.7±0.10
UNx+DM	319±13.4 [a, b]	356±20.0 [a, b]	355±12.8 [a, b]	1.7±0.17 [a]	3.1±0.30 [a, b]	5.7±0.91 [a, b]
UNx+DM+NTU281	320±6.7 [a, b]	350±10.3 [a, b]	377±14.3 [a, b]	2.3±0.25 [a, b, c]	2.8±0.36 [a, b]	3.3±0.25 [a, b, c]

Data represents mean ± SEM, n=4-7 per group. Significance (P<0.05) is indicated in comparison to normal (a), UNx(b), untreated DM (c).

Titles and legends

Figure 1. NTU281 Distribution. The kidney distribution of dansyl labelled NTU281 (Green) in both transverse and longitudinal planes from an intra parenchymal renal cannula inserted 28 days previously with 24 hours drug delivery from an implanted osmotic pump (A). Inset shows effect of cannulation on renal morphology on a Masson's Trichrome stained slide at 1 month. Quantification of fluorescence in comparison to the contralateral kidney in both longitudinal (B) and transverse (C) planes.

Figure 2: Hyperglycaemia,kidney function and drug delivery. The volume of drug delivered per month was calculated from residual volumes in the pump (i). Insulin implants required to control blood glucose to 10-25 mmol/L were averaged for each experimental group (ii). The average blood glucose of each animal over the monitoring period was determined (iii). Changes in body weight (g) were calculated by subtracting the initial body weight from the final body weight at each time point

(iv). Kidney function was assessed by measuring serum creatinine concentration (μmol/L) (v). 24-hour albumin excretion (mg) was used to assess glomerular damage (vi). White circles = normal, black circles = UNx, white squares = untreated DM, black squares = NTU281 treated DM. Data represents mean ± SEM, n=4-7 per group. Significance (P<0.05) is indicated in comparison to normal (a), UNx(b), untreated DM (c) and NTU281 treated DM (d).
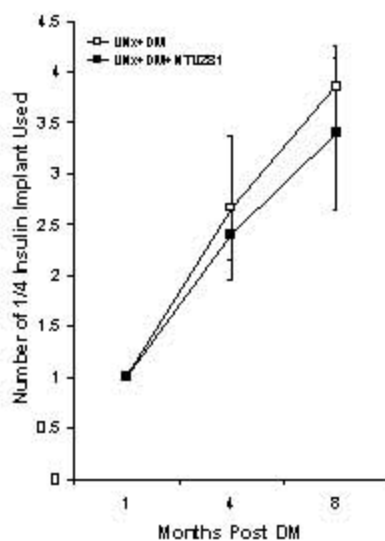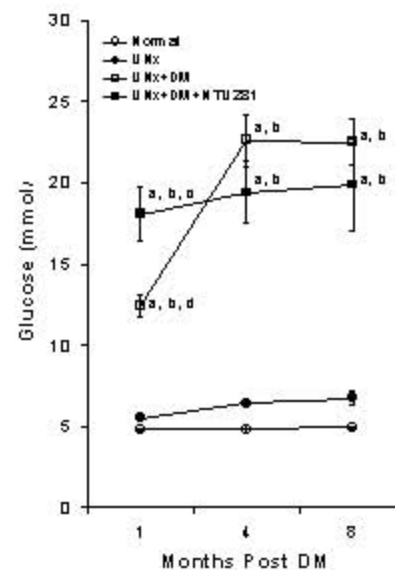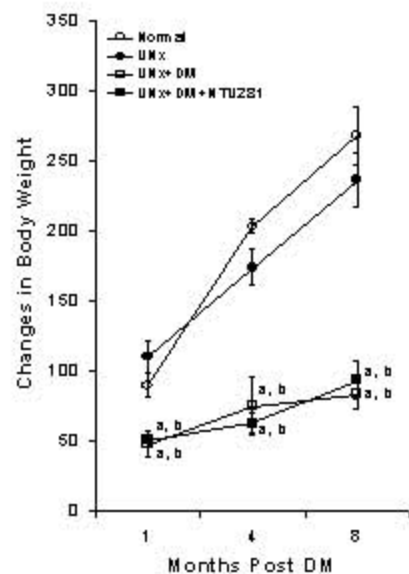
Figure 3: TG inhibition. The effectiveness of NTU281 to reduce TG activity was assessed by measuring *in situ* TG activity using multiphase image analysis at 1, 4 and 8 months post STZ (i). Representative TG *in situ* activity confocal microscope images at 8 months for normal (A), UNx (B), DM (C) and DM+NTU281 (D) kidneys with TG activity shown in red (ii). Inhibition was confirmed by determining TG catalysed ε-(γ-glutamyl) lysine crosslink staining again using multiphase image analysis (iii). White circles = normal, black circles = UNx, white squares = untreated DM, black squares = NTU281 treated DM. Data represents mean ± SEM, n=4-7 per group. Significance (P<0.05) is indicated in comparison to normal (a), UNx(b), untreated DM (c) and NTU281 treated DM (d).

Figure 4: Masson's trichrome staining. 4μm thick sections from 1month (A-D), 4 months (E-H) and 8 months (I-L) post induction of hyperglycaemia were stained for Masson's trichrome (40× magnification).

Figure 5: Glomerular Electron Microscopy. Paraffin embedded tissue from 8 month experimental groups was post fixed in gluteraldehyde and observed by transmission electron microscopy at 2,600 (A) and 20,000 (B) magnification. Glomerular basement membrane (GBM) thickness was measured by computerised

morphometric analysis by a pathologist blinded to experimental groups (C). Data represents mean GBM thickness ± SEM. *=Significance from normal (p<0.05)

Figure 6: Glomerulosclerosis and tubulointerstitial scarring. Glomerulosclerosis (i) and tubulointerstitial scarring (ii) were assessed by multiphase image analysis of Masson's trichrome stained sections. 20 glomeruli (400× magnification) or 10 cortical tubulointerstitial fields (200× magnification) were analysed respectively per section. White circles = normal, black circles = UNx, white squares = untreated DM, black squares = NTU281 treated DM. Data represents mean ± SEM, n=4-7 per group. Significance (P<0.05) is indicated in comparison to normal (a), UNx(b), untreated DM (c) and NTU281 treated DM (d).

Figure 7: Quantification of collagen I, III, IV and α-SMA immunostaining. Kidney levels of collagen I (i), collagen III (ii), collagen IV (iii) and α-SMA (iv) staining (Figure 6) were assessed by multiphase image analysis of 10 fields per section. White circles = normal, black circles = UNx, white squares = untreated DM, black squares = NTU281 treated DM. Data represents mean ± SEM, n=4-7 per group. Significance (P<0.05) is indicated in comparison to normal (a), UNx(b), untreated DM (c) and NTU281 treated DM (d).

Figure 8: Immunofluorescent staining of collagen I, III, IV and α-SMA in kidneys 8-month post hyperglycaemia. Collagen I staining (A-D) was performed on cryostat sections with collagen III (E-H), collagen IV (I-L) and α-SMA (M-P) on paraffin sections. Fields were acquired at 200× magnification on a Olympus BX61 fluorescent microscope using a FITC and DAPI filter sets.

Figure 9: Northern blot analysis of collagen I, III and IV mRNA. mRNA levels of collagen I (i), collagen III (ii) and collagen IV (iii) were assessed by Northern blot analysis using volume densitometry measurements normalised to the house keeping gene cyclophilin (iv). Some displayed autoradiographs are over exposed for diseased groups to allow clear visualisation in normal kidneys White circles = normal, black circles = UNx, white squares = untreated DM, black squares = NTU281 treated DM. Data represents mean optical density ± SEM, n=4-7 per group. Significance (P<0.05) is indicated in comparison to normal (a), UNx(b), untreated DM (c) and NTU281 treated DM (d).

A

0.58 mm bore cannula

2mm

Longitudinal section

Transverse section

20x   20x

Contralateral   +Dansyl 281

20x   Contralateral

20x   +Dansyl 281

200x   Contralateral

200x   +Dansyl labelled 281

B

Longitudinal Fluorescence

Kidney + Dansyl labelled 281

Mean OD = 0.23 U

Top   Bottom

Contra lateral Kidney

Mean OD = 0.01 U

Top   Bottom

C

Transverse Fluorescence

Kidney + Dansyl labelled 281

Mean OD = 0.21 U

Left   Right

Contra lateral Kidney

Mean OD = 0.009 U

Left   Right
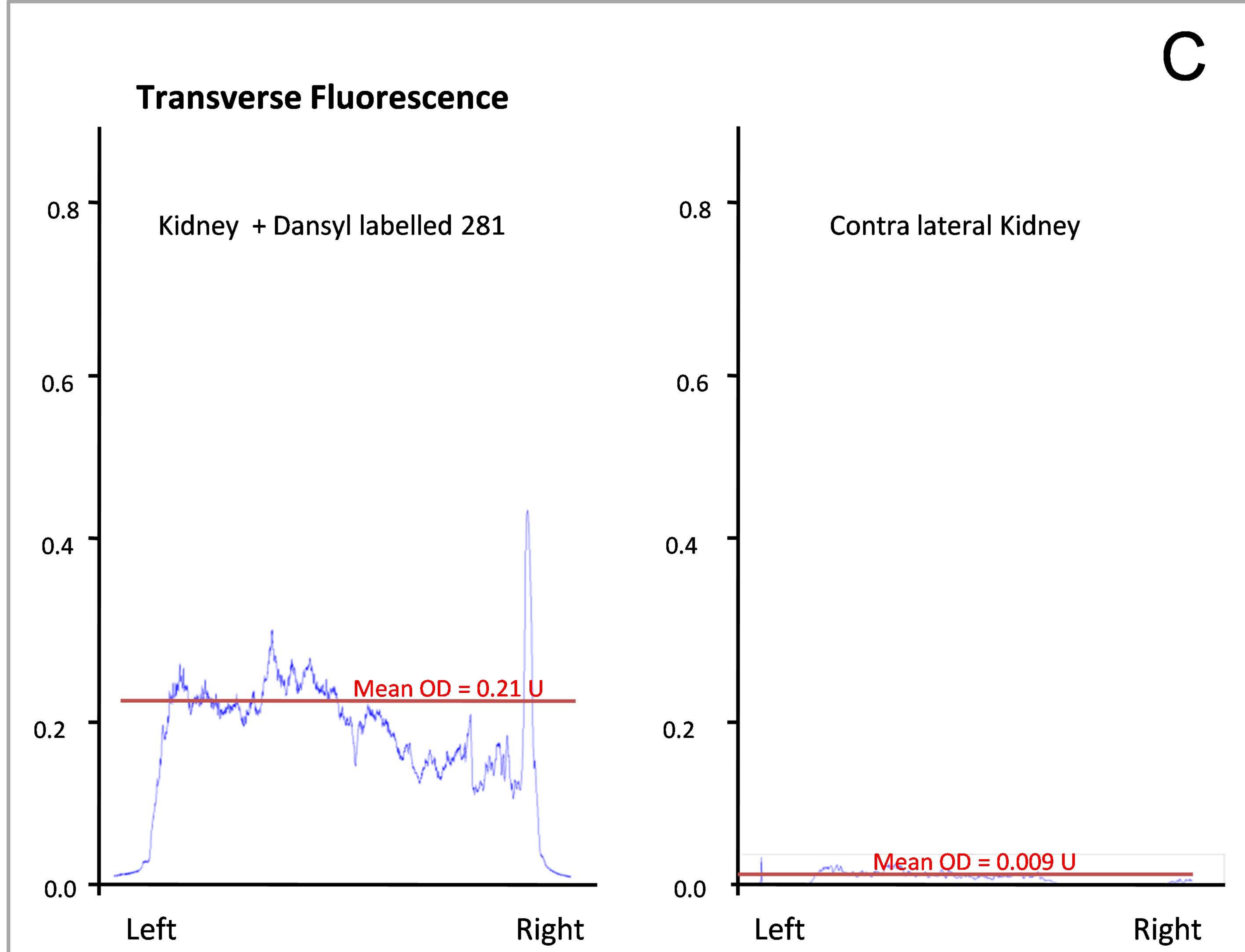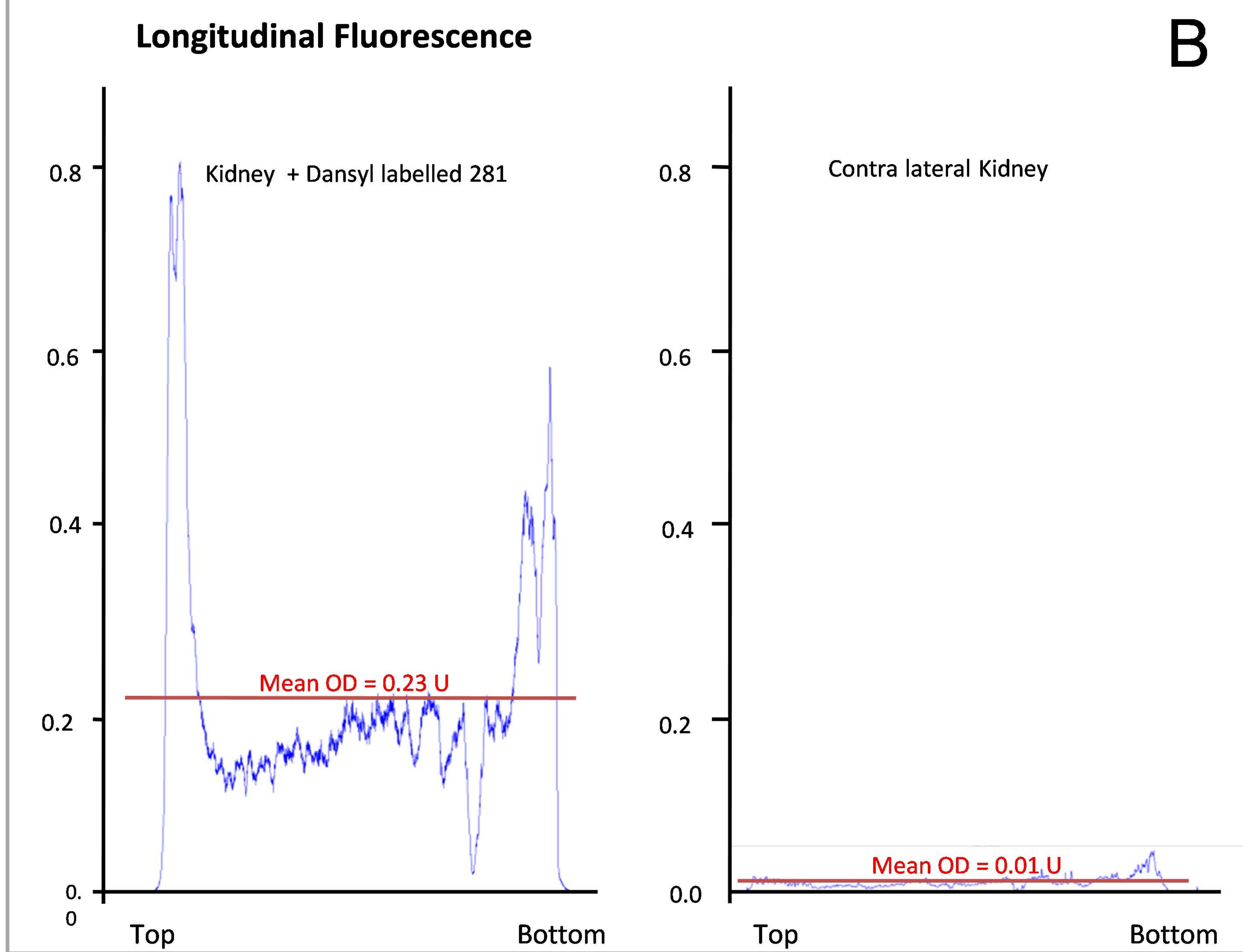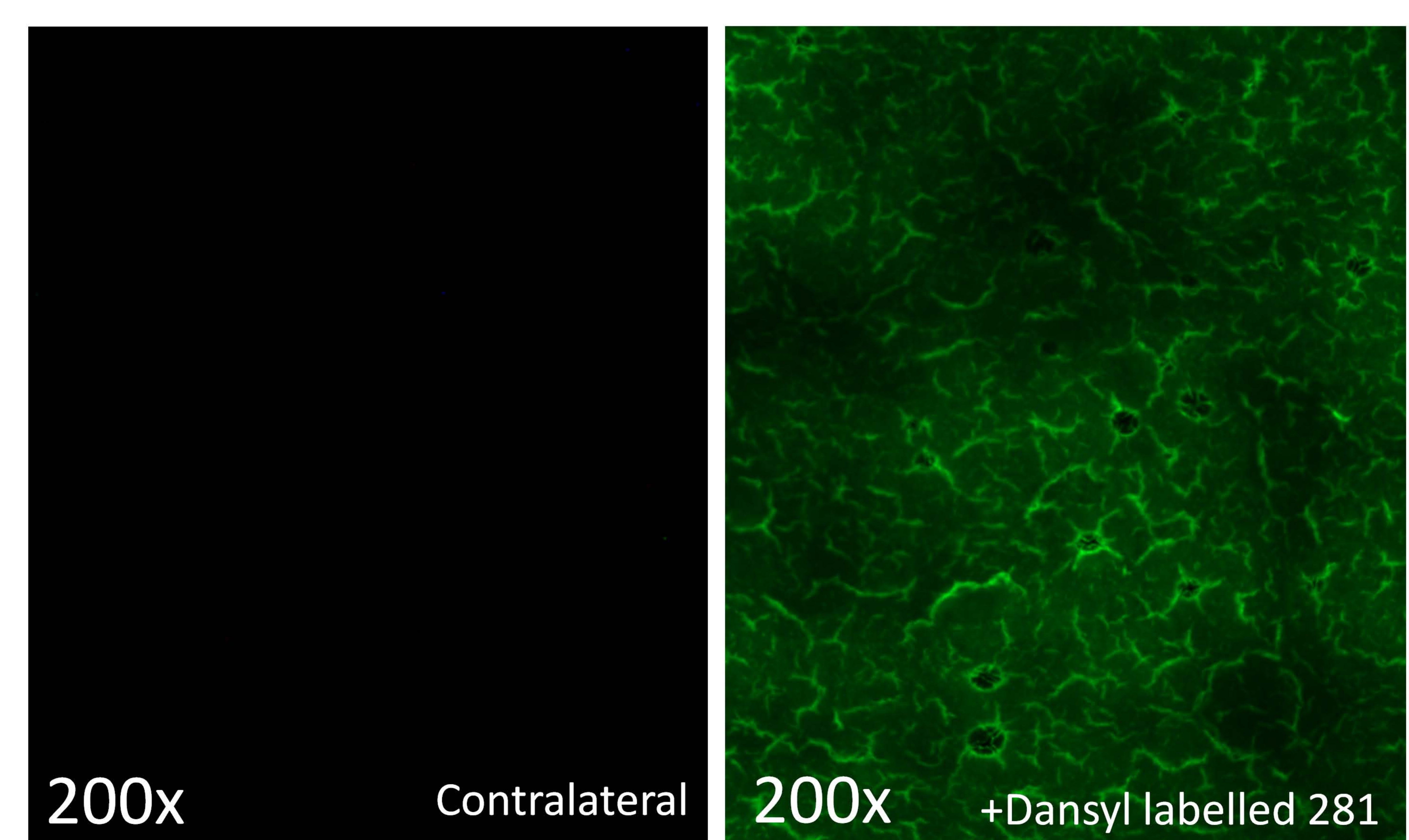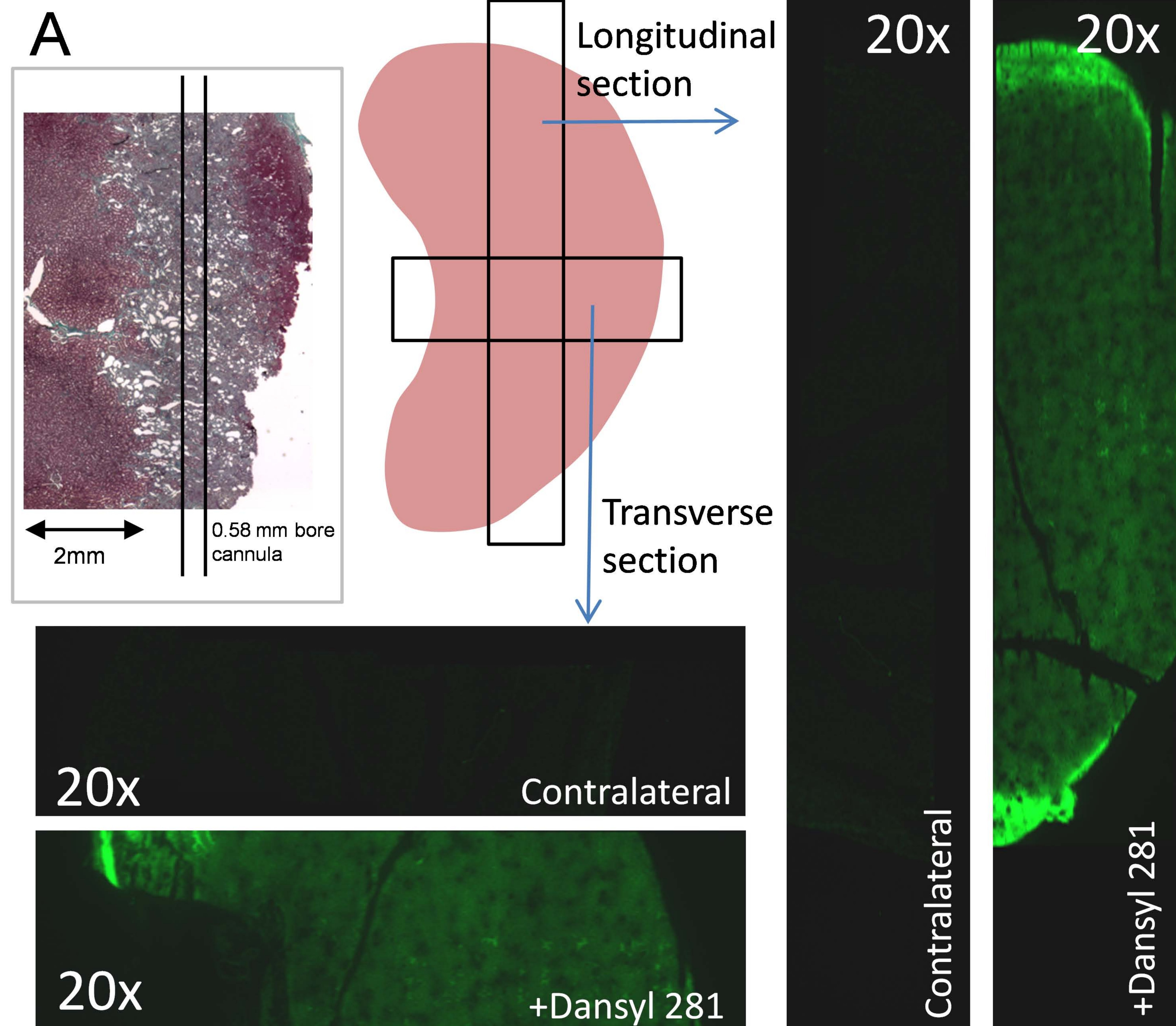
i. NTU281 delivery
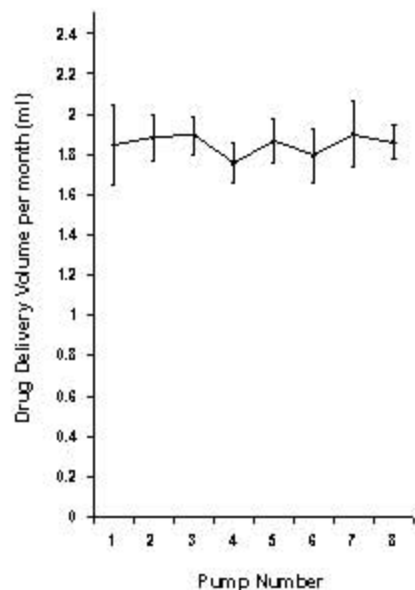
ii. Insulin dose

iii. Blood glucose

iv: Body weight gain

v: Serum creatinine
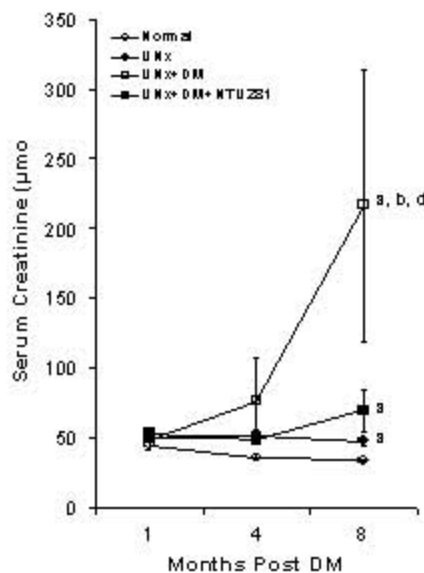
vi: 24-hr albuminuria
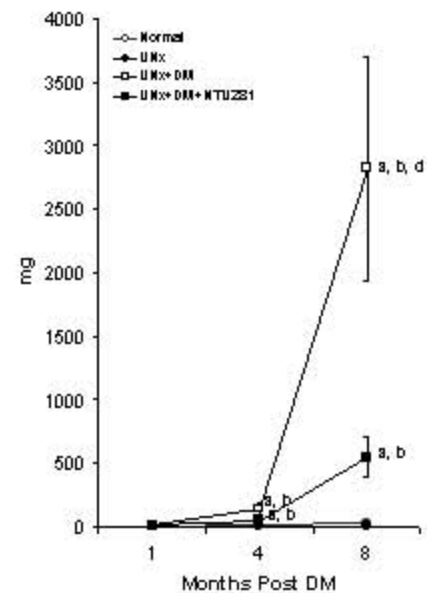
i: *In situ* TGase activity
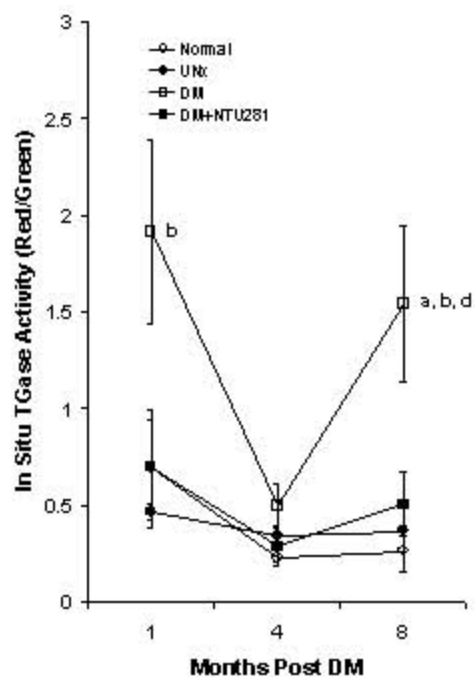
iii: ε-(γ-glutamyl)-lysine crosslink
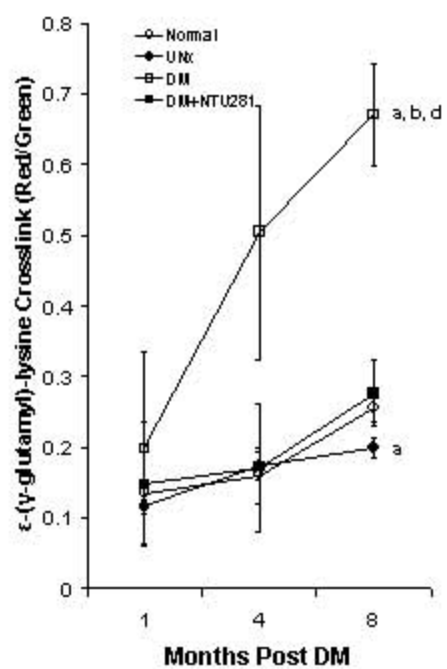
ii: *In situ* TGase activity
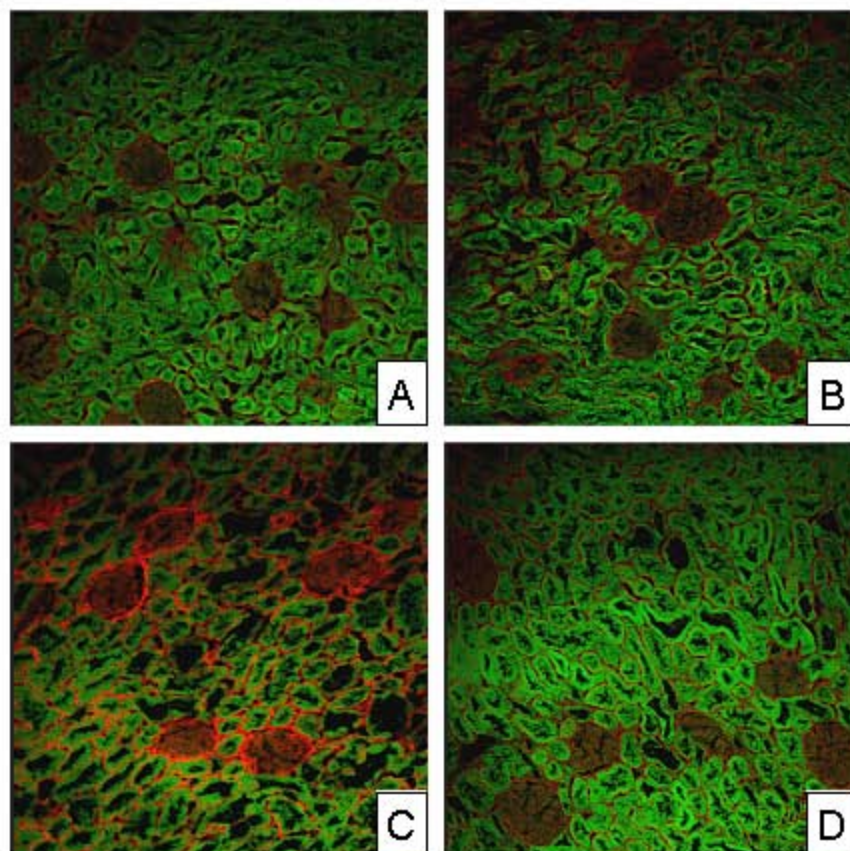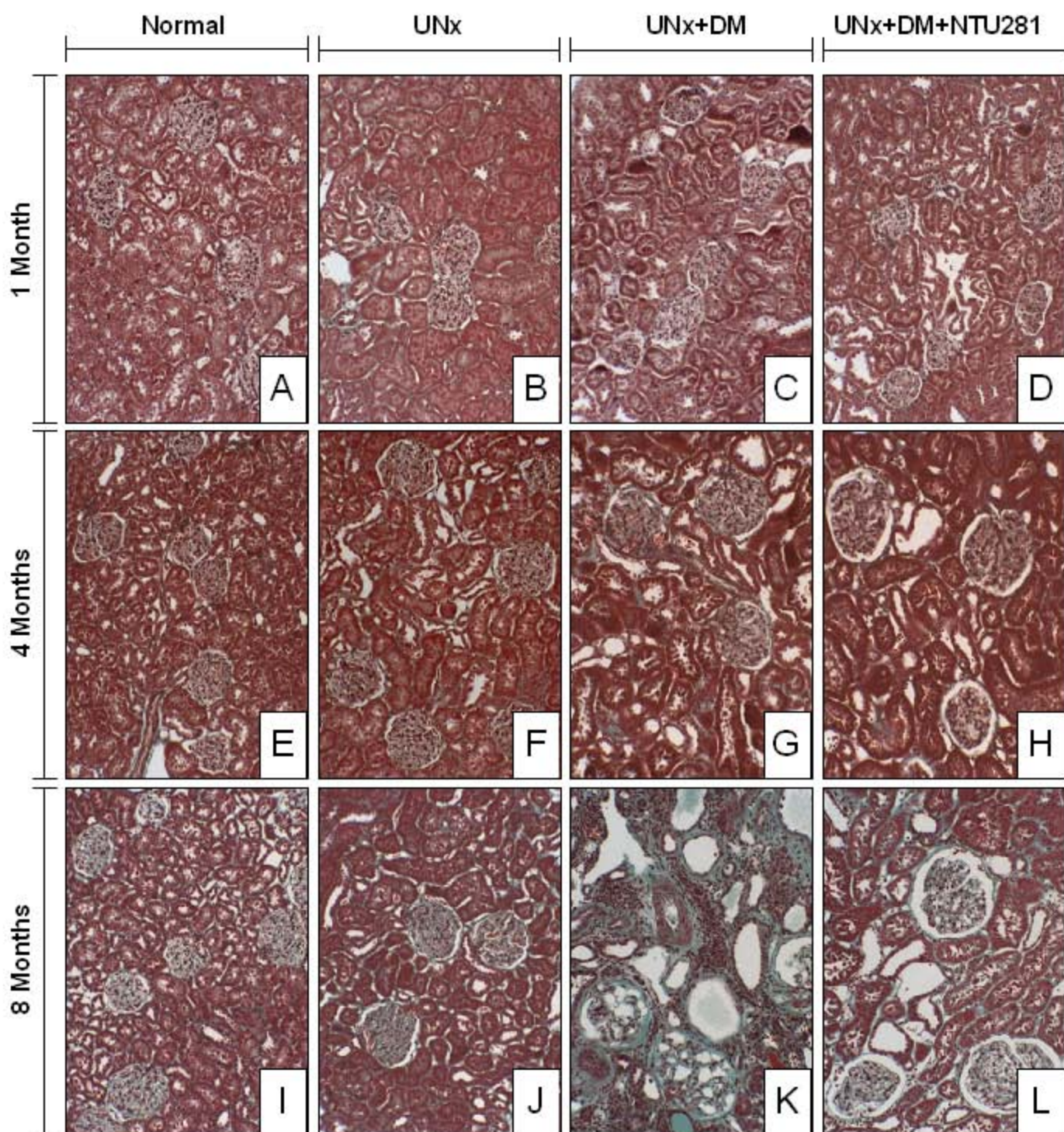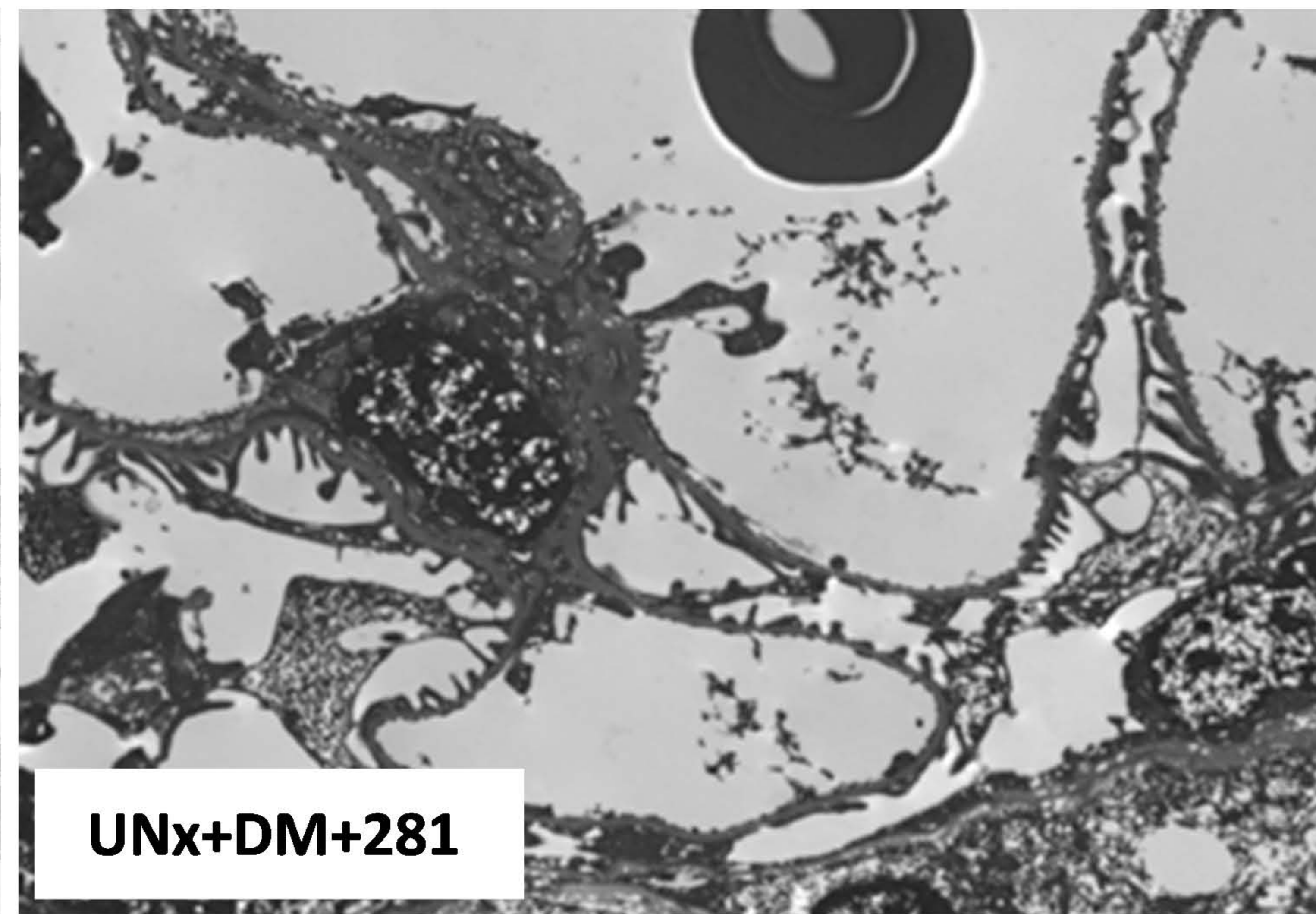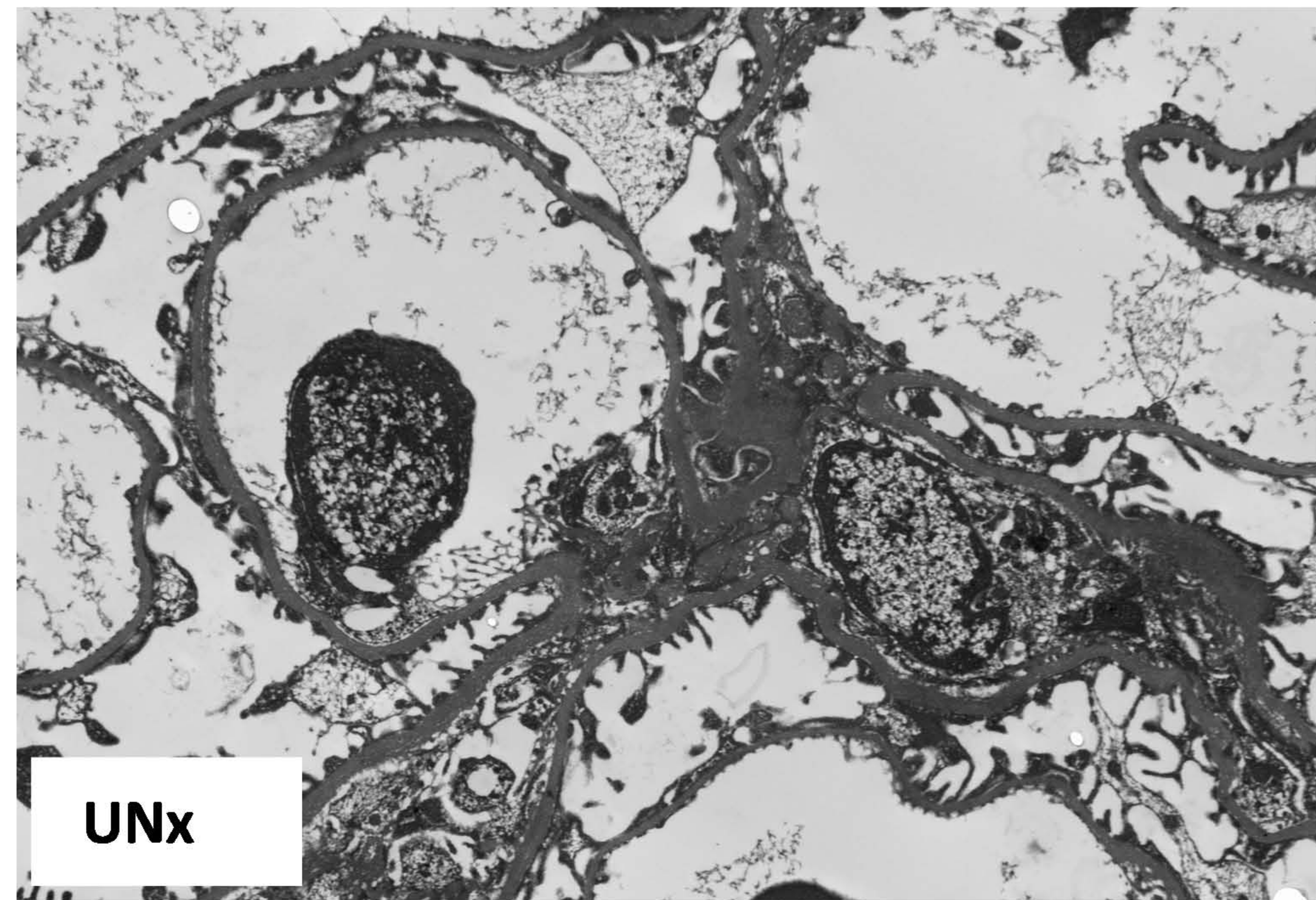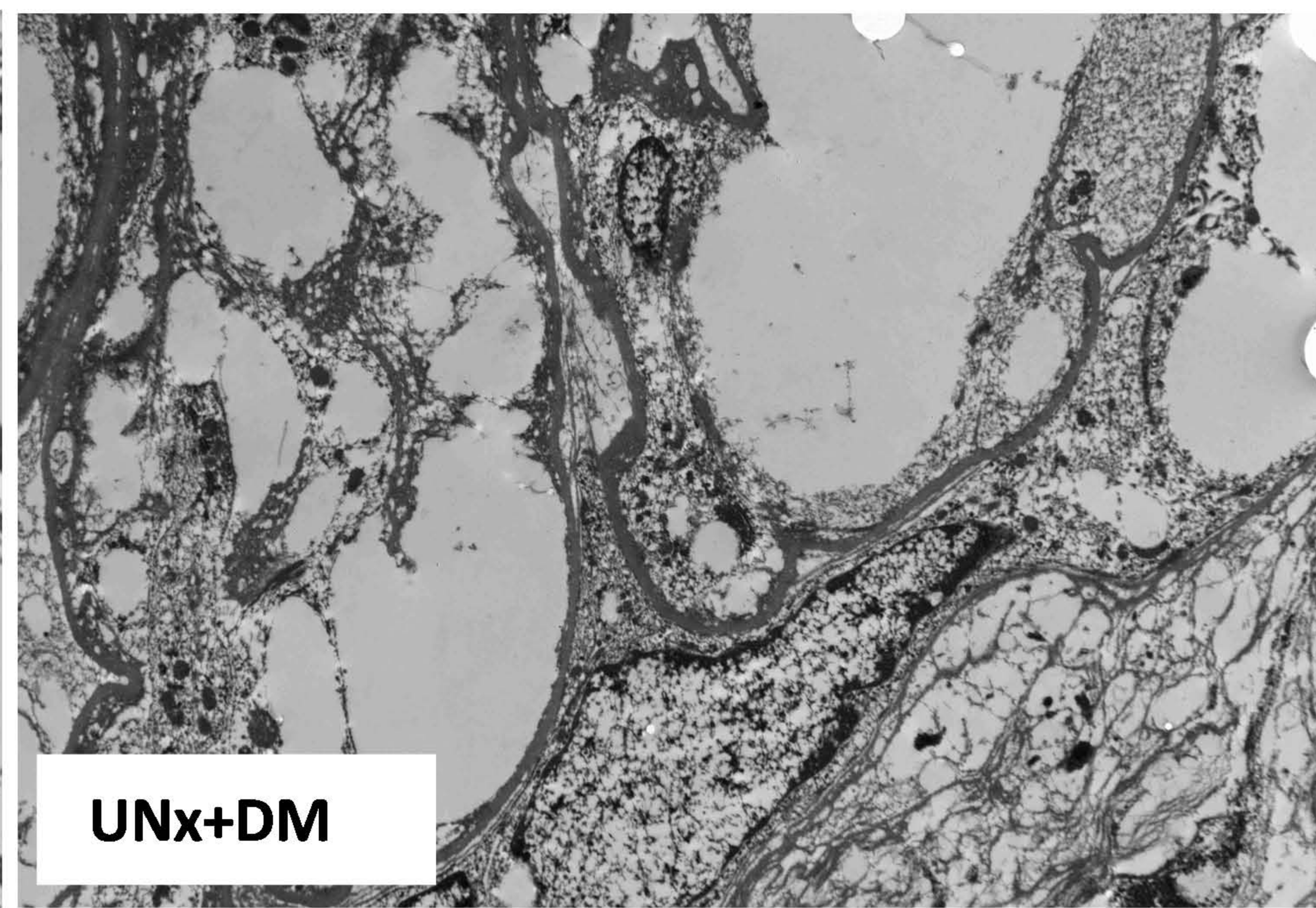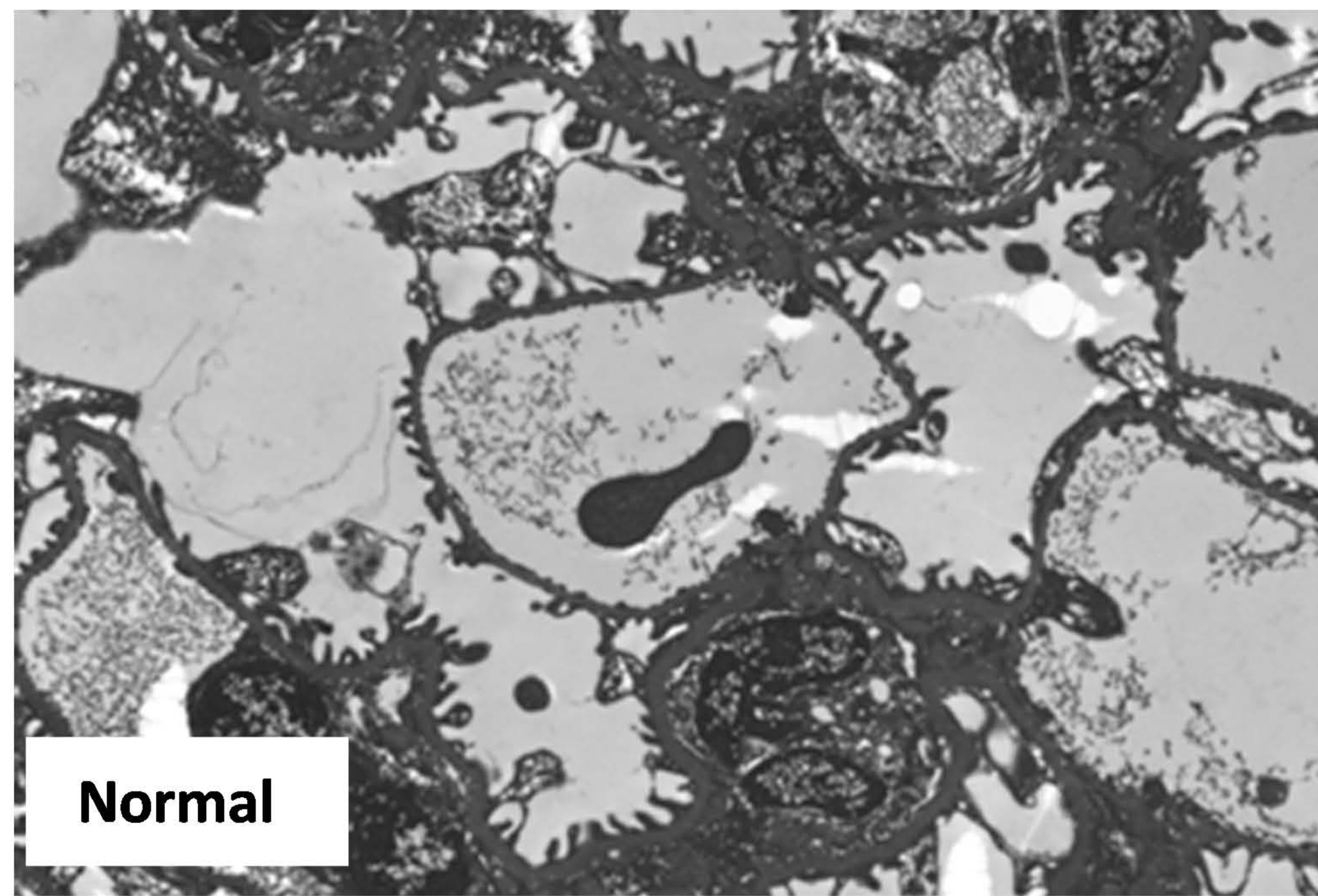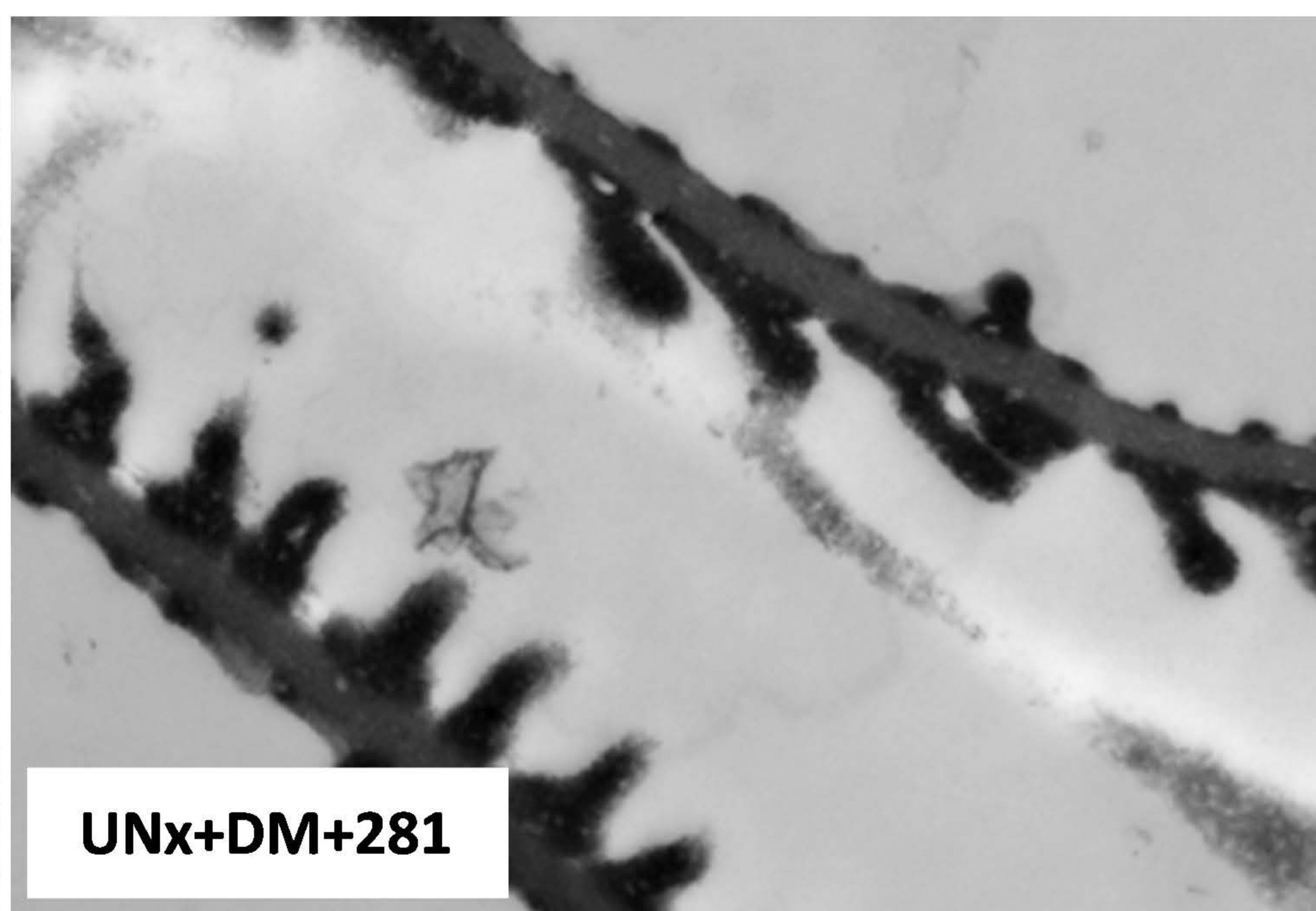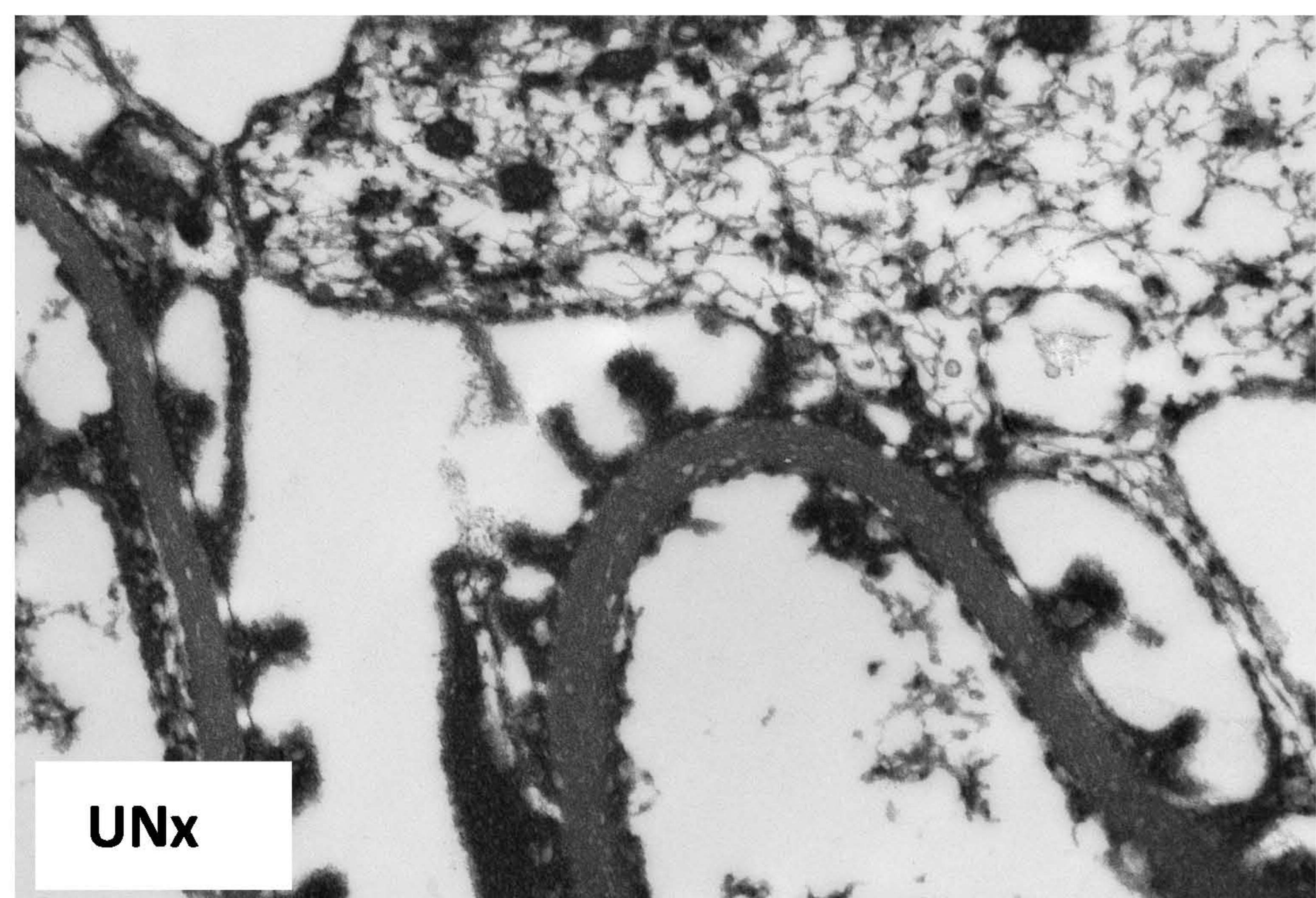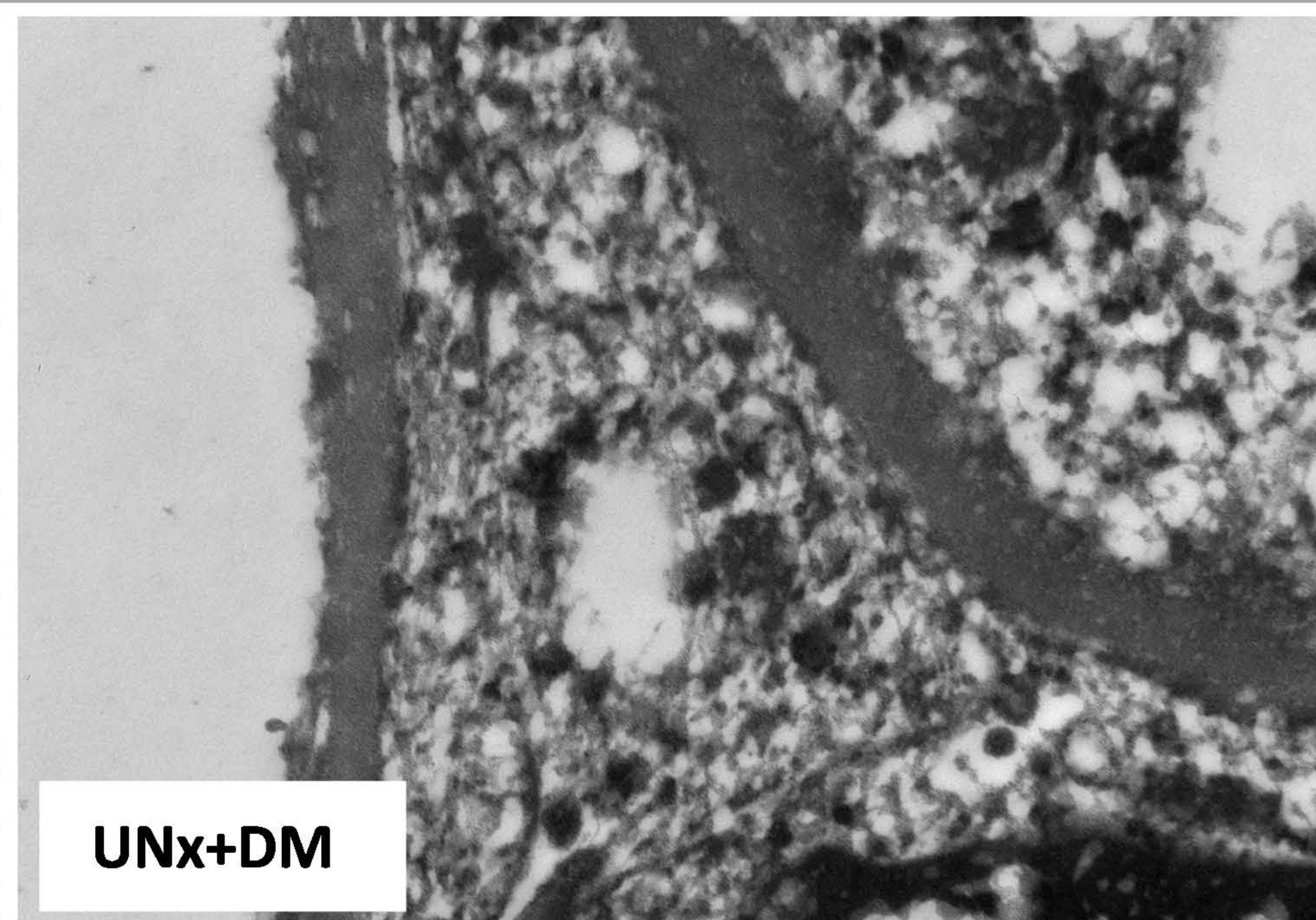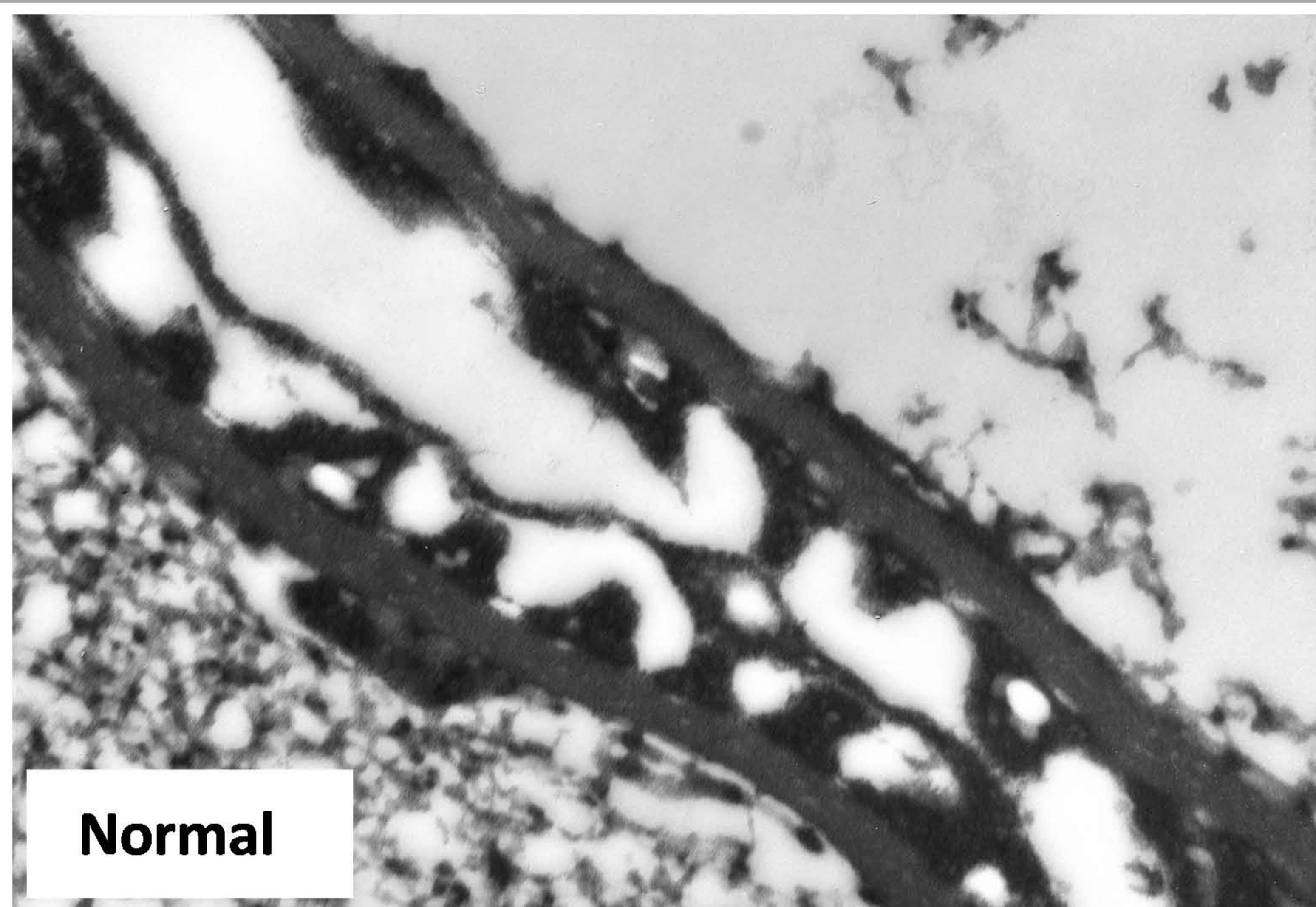
	Normal	UNx	UNx+DM	UNx+DM+NTU281
1 Month	A	B	C	D
4 Months	E	F	G	H
8 Months	I	J	K	L

A

Magnification 2600x

Normal

UNx+DM

UNx

UNx+DM+281

B

Magnification 20 000x

Normal

UNx+DM

UNx

UNx+DM+281

C

Glomerular Basement Membrane thickness (uM)

Normal   UNx   DN+UNx   DN+UNx+281

i: Glomerulosclerosis

Y-axis: Glomerular Scarring Index (Blue/Red)
X-axis: Months Post DM

Legend:
- Normal
- UNx
- DM
- DM+NTU281

Labels: a,b,d; a,b,d; a,b,d; b,d

ii: Tubulointerstitial scarring

Y-axis: Tubular Scarring Index (Blue/Red)
X-axis: Months Post DM

Legend:
- Normal
- UNx
- DM
- DM+NTU281

Labels: a,b,d; a,b,d; b,d
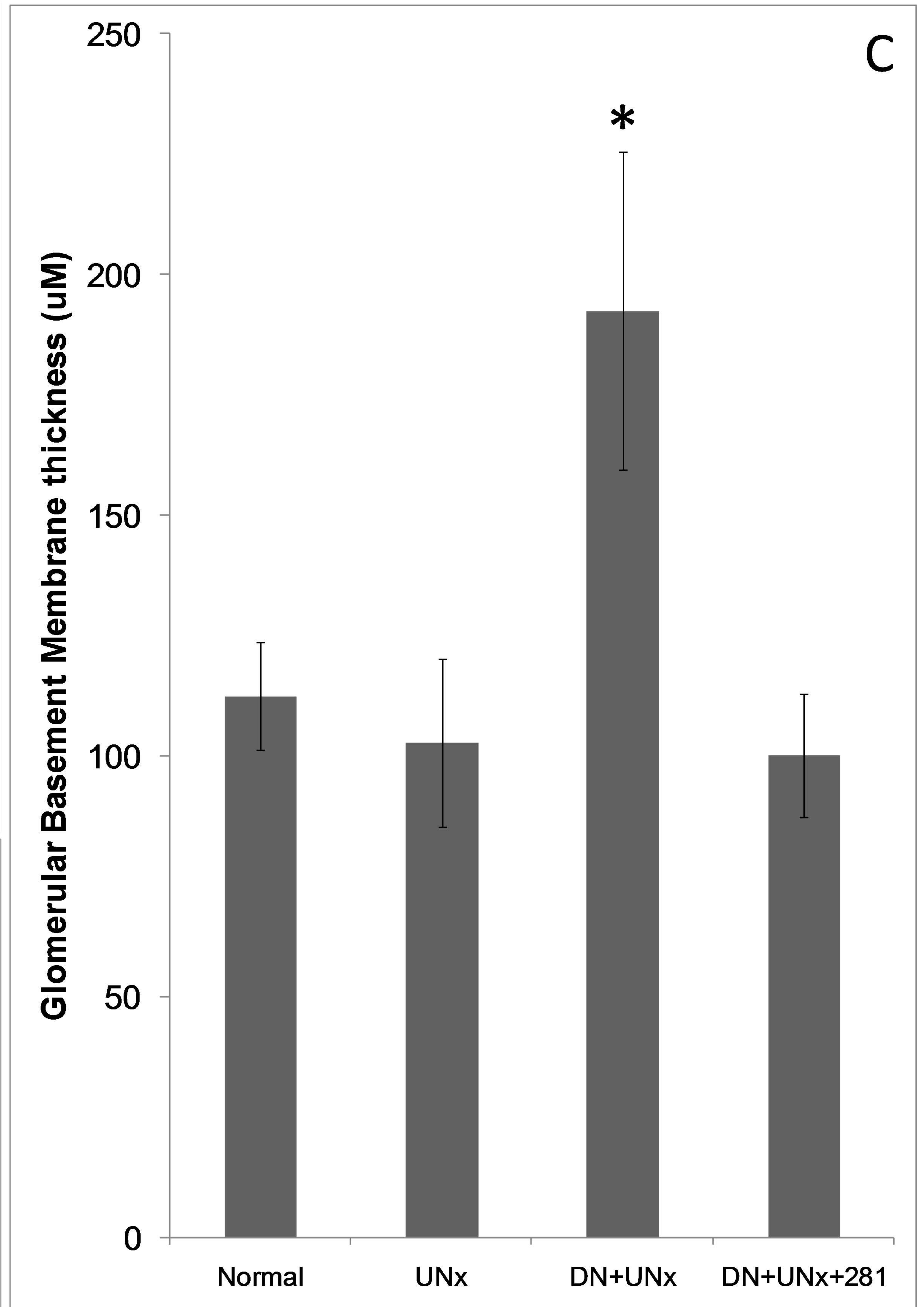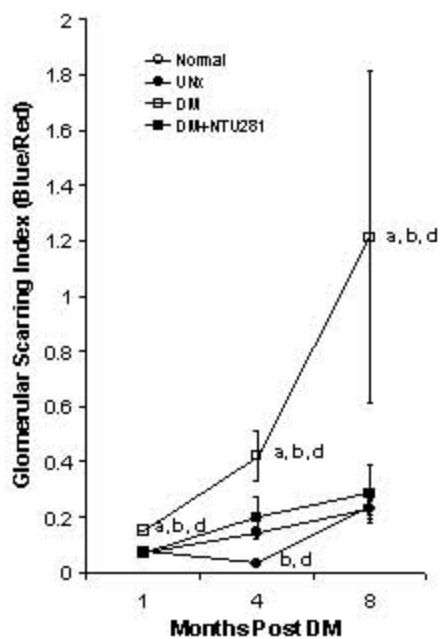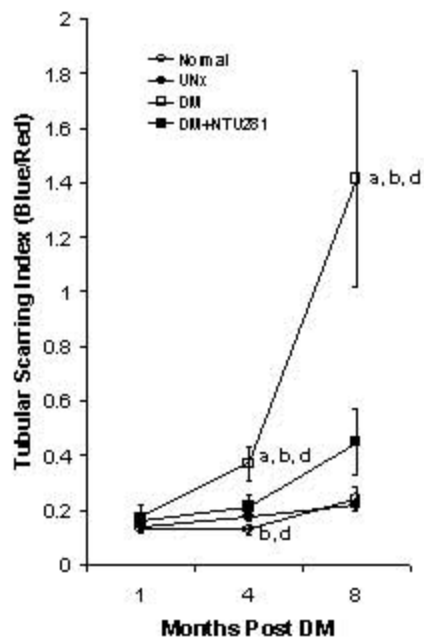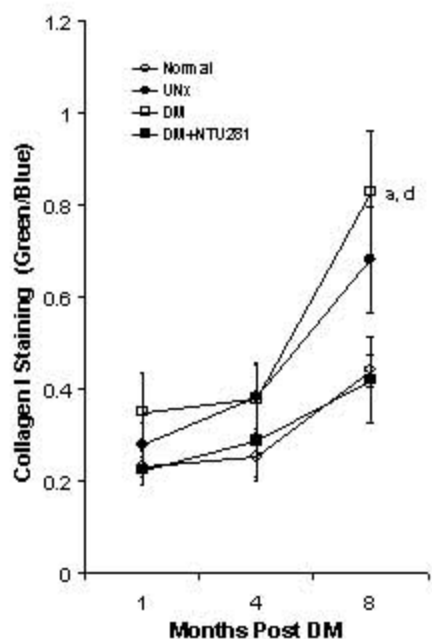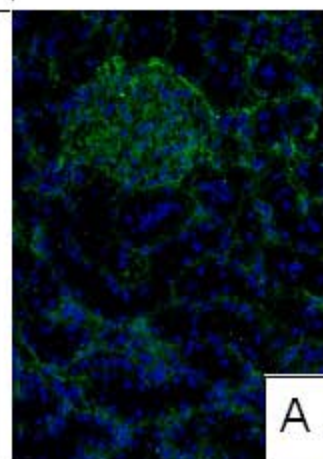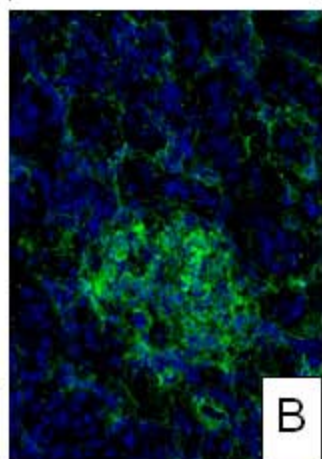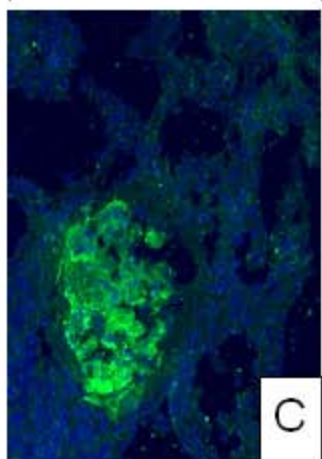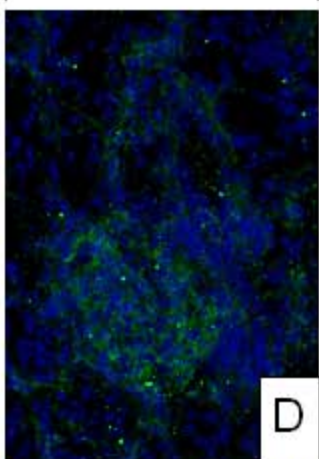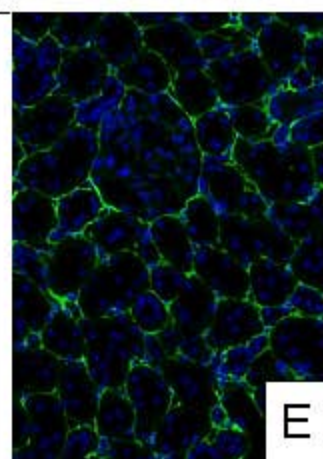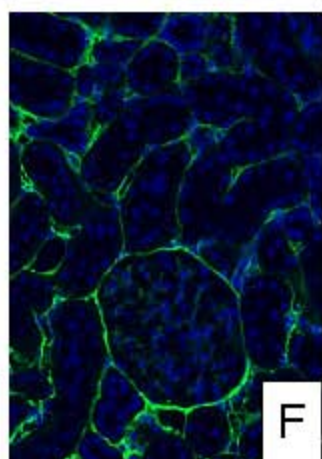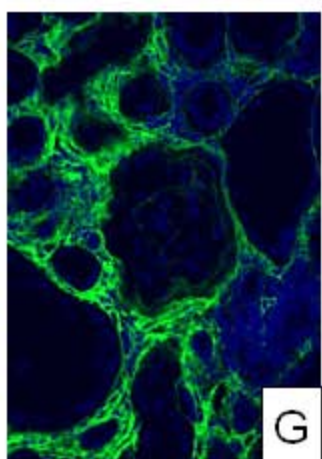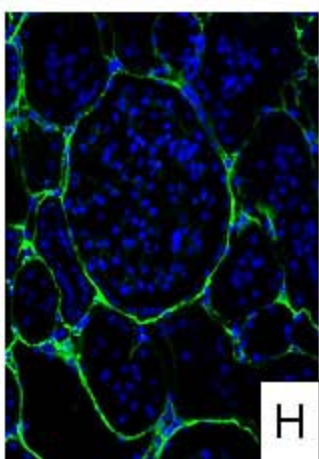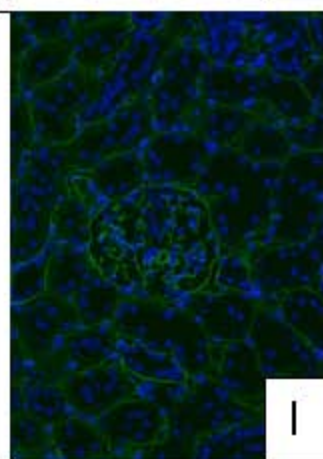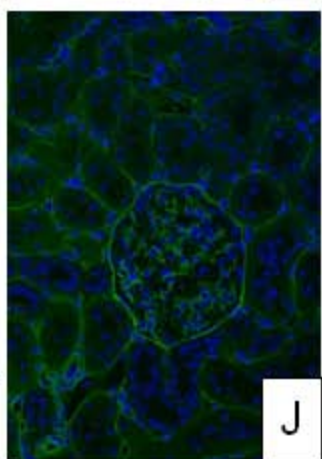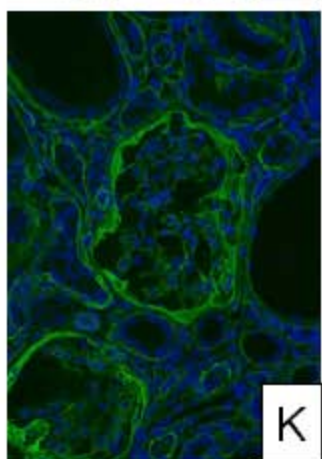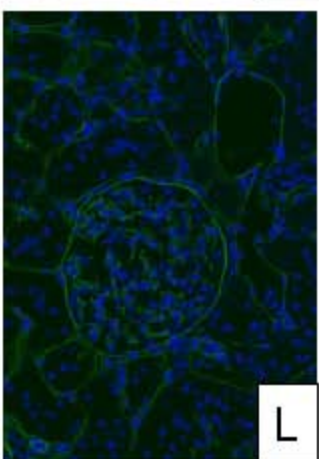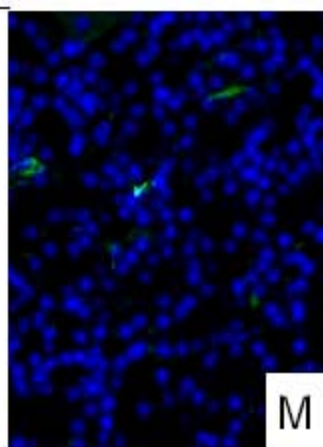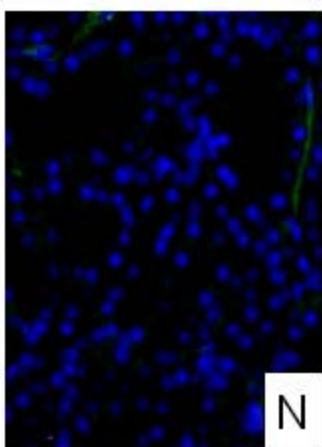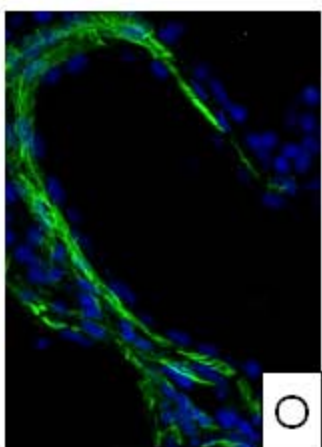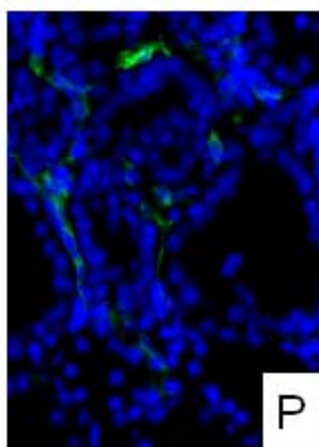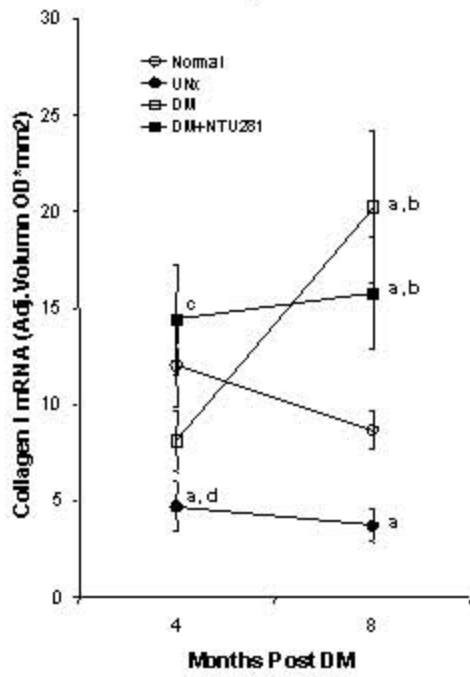
i: Collagen I

ii: Collagen III

iii: Collagen IV

iv: α-smooth muscle actin

i: Collagen I

Collagen I mRNA (Adj.Volumn OD*mm2)

Legend: Normal, UNx, DM, DM+NTU281

ii: Collagen III

Collagen III mRNA (Adj.Volumn OD*mm2)

Legend: Normal, UNx, DM, DM+NTU281

iii: Collagen IV

Collagen IV mRNA (AdjVolumn OD*mm2)

Legend: Normal, UNx, DM, DM+NTU281
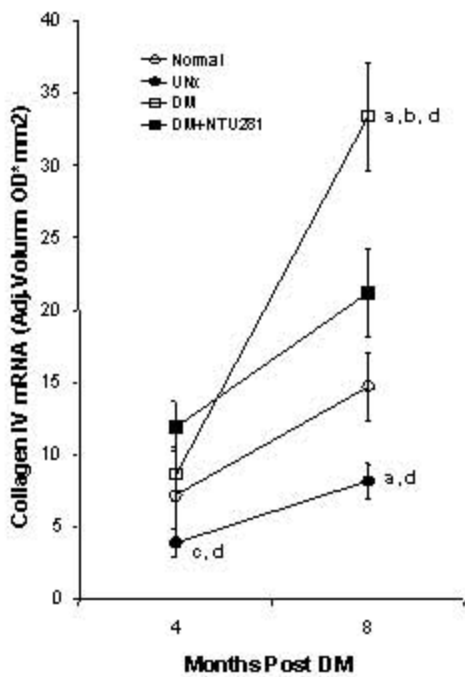
iv: Northern blot analysis of 8-month kidney tissue

Normal   UNx   DM   DM+NTU281

Collagen I (4.8 kb)

Collagen III (5.4 kb)

Collagen IV (6.5 kb)

Cyclophilin (0.74 kb)